INVESTIGATION OF LIGNIN NANOCAPSULES UPTAKE IN PLANTS

Franco Cheli (521160 UTU)

Master's thesis
University of Turku
Faculty of Medicine
16/09/2021
Master's degree programme in Biomedical Sciences
Specialization field: Biomedical Imaging
Credits: 20 ECTS
Supervisor: Sara Falsini, PhD
Passed:
Grade:

Abstract

The interest of the scientific community in nanotechnology has been growing significantly in the last decades, resulting in the development of new nanomaterials and nanoparticles which can find a wide variety of applications, ranging from materials science to biomedicine.
Researchers have recently started to investigate the engineering of nanoparticles which can be used as pest controls or cargo deliverers to improve agriculture yield and to reduce the use of pesticides and fertilizers in favour of more sustainable approaches.

The present work aims to contribute to the advancement of nanotechnology in the context of sustainable agriculture by evaluating the viability of lignin nanocapsules (NCs) produced by ultrasonication as nanovectors (NVs) for bio-active compounds in plants.
Different light microscopy and electron microscopy techniques have been used to image the roots of *Eruca sativa*, *Eragrostis tef* and *Arabidopsis thaliana* seedlings exposed to the NCs in several experiments which investigated the toxicity and uptake extent of the particles.

The study revealed that low dilutions of the raw NCs emulsion have toxic effects on roots cells and hair and required the administration of highly diluted emulsions to avoid detrimental effects. However, the imaging revealed no evidence of NCs uptake and internalization in lively cells in any of the conducted experiments. As a consequence, we can assert that the main reason for the missed uptake must reside in the size of the particles, revealing the necessity of developing a different production process which could yield smaller particles.

Keywords: agriculture, lignin, microscopy, nanocapsules, nanomaterials, nanoparticles, nanotechnology.

Abbreviations

NM - Nanomaterial

NP - Nanoparticle

NV - Nanovector

NC - Nanocapsule

FNC - Fluorescent nanocapsule

NS - Nanosphere

LS - Linsmaier and Skoog

RI - Refractive index

LSFM - Light sheet fluorescence microscopy

CLSM - Confocal laser scanning microscopy

2PEFM - Two-photon excitation fluorescence microscopy

TEM - Transmission electron microscopy

DLS - Dynamic light scattering

PMT- Photomultiplier

PI - Propidium iodide

Table of contents

1. Introduction

1.1 Nanotechnology

Nanotechnology is a rapidly developing field of applied science and technology which uses matter on an atomic or molecular scale for the fabrication of nanomaterials (NMs) with peculiar physical and chemical properties dependant on their size, structure and chemical composition (Salata, 2004). The majority of authors consider nanomaterials objects which have at least one dimension smaller than 100 nanometres (US Food and Drug Administration), while others (Gurr et al., 2005; Jeevanandam et al., 2018; Briolay et al., 2021) refer to "nanomaterials" to any particle within 1 to 1000nm size. Nanomaterials can range from simple, pure inorganic metallic, ceramic or semiconductor nanoparticles (NPs), to carbon or organic, polymeric and lipidic nanoparticles or various combinations of the latter with the possible loading of cargos in their inner core or functionalised groups on their outer shell. Depending on their nature (Figure 1), nanomaterials can be used for the design and engineering of new materials, drug delivery vectors for cancer therapy, biosensors, fluorescent probes for biomedical imaging (e.g. quantum dots), remedies for environmental pollution, constituents of electronic components and energy harvesting and storing devices thanks to their large surface area, optical behaviour and catalytic properties (Khan et al., 2019).

Both naturally-occurring and synthetic nanoparticles and nanomaterials can show toxicity for biological systems due to their ability to permeate cell membranes, eventually accumulating in certain tissues and interact with biological molecules such as proteins and nucleic acids, arising the issue of their impact upon environmental release (Taghavi et al., 2013; Bahadar et al., 2016). Their toxicity can be addressed to their interaction with biological molecules which depends on their size, shape, curvature, surface charge, free energy and the eventual presence of functionalized groups causing unfolding of proteins, fibrillation, crosslinking, oxidative damage (Gurr et al., 2005) and deactivation of enzymes as well as the possible release of toxic ions as a consequence of the thermodynamic properties of the surrounding medium in favour of their dissolution (Xia et al., 2008).

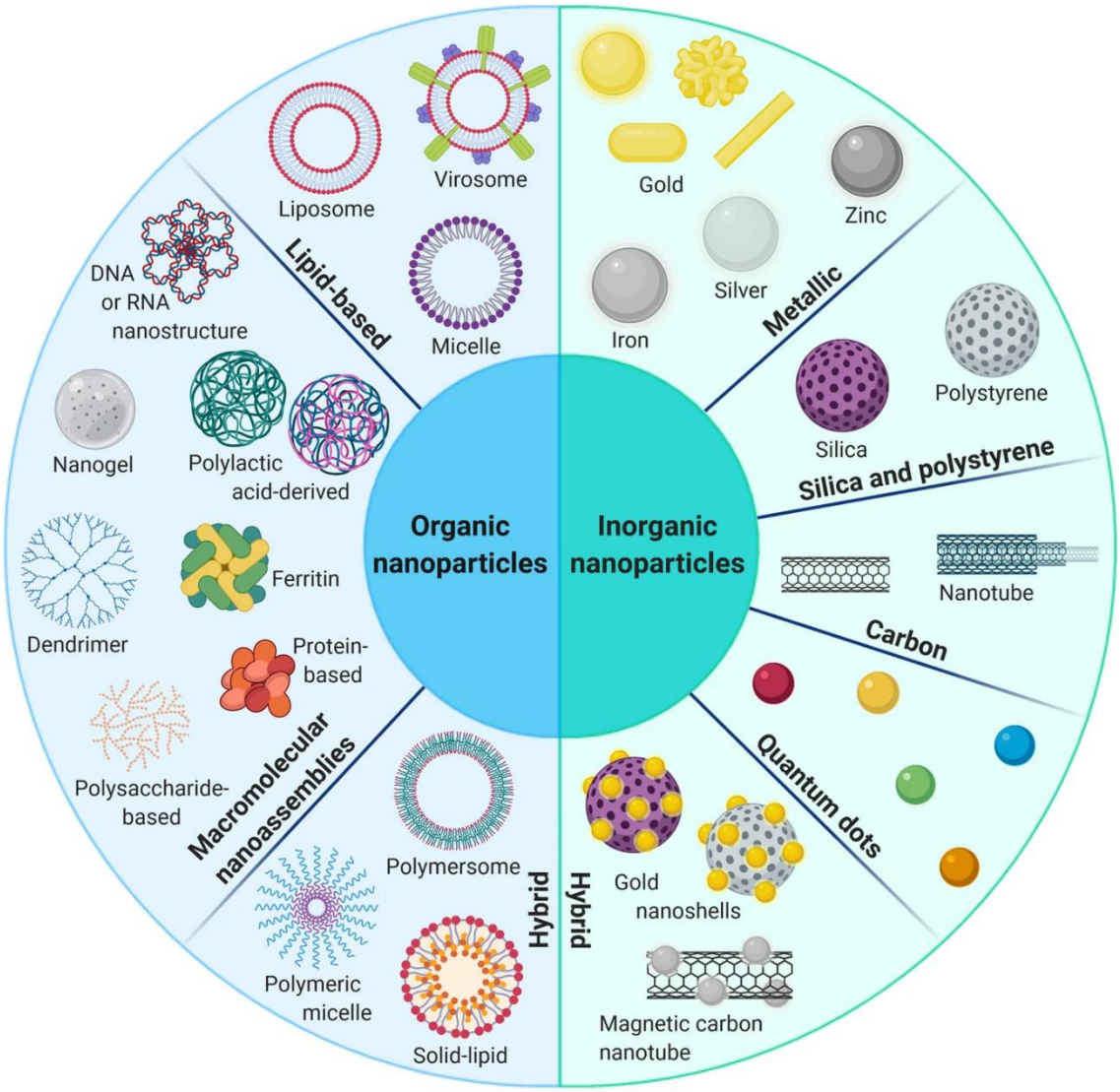

Figure 1. Types of nanoparticles. Inorganic NPs show high stability and low biodegradability and their chemical and optical properties make them suitable for biomedical imaging and theranostics. Organic NPs are less stable in biological environments, but have low toxicity and high biocompatibility, representing possible vectors for drugs by the functionalization of their outer shell or inner core. Image from Briolay et al., 2021.

1.2 Nanovectors applications

The interest in nanoparticles and their applications in cancer and other diseases therapy has been rising significantly in the past decades among the scientific community as many *in vitro* and *in vivo* studies revealed a significant efficacy of drug delivery by artificially designed nanovectors (NVs) which can release their cargo to target cells or tissues (Faveeuw and Trottein, 2014; Shi et al., 2017). This application field of nanotechnology is nowadays referred to as “nanomedicine” (Soares et al., 2018).

Specific targeting and delivering is a key aspect of cancer treatment which aims to maximize the therapy outcome while minimizing the off-target detrimental side effects

(Briolay et al., 2021). Recent studies demonstrated that hybrid poly(methacrylic acid)-grafted gold nanoparticles can be successfully used as radiosensitizers in radiotherapy, resulting in a lower radiation dose for the patient and subsequently reduced side effects. In addition, the potential to add anticancer compounds such as doxorubicin onto the polymeric surface of the particles will allow the combination of radiosensitization and chemotherapy (Le Goas et al., 2019).

To mention another example, silica mesoporous nanocarriers loaded with iron and gallic acid have been engineered to selectively dissolve into acidic tumour cells, releasing their Fe3+ and gallate which, by a chelation reaction, produce GA-Fe nanocomplex *in situ* which can catalyse the formation of hydroxyl radical, causing fatal oxidative damage to tumours cells (Zhou et al., 2021).

Recent studies (Zhang et al., 2016) found that plant-produced exosomes (PDENs, plant-derived edible nanoparticles) in grapes, ginger, carrots and other plants are similar to exosomes derived from mammalians and can be easily isolated with an eco-friendly procedure (Quesenberry et al., 2015) and used as nanovectors to deliver mRNAs, miRNAs and bioactive molecules into animal cells, opening up a novel approach in nanomedicine.

The suitability of a nanovector in disease treatment depends on its capability of increasing drug solubility and half-life, improve its bioavailability and decrease its off-target and side effects while at the same time being able of crossing biological membranes. As a consequence, an effective nanovector can selectively target the tumour tissue and accumulate the drug within its cells, increasing the specificity and efficacy of the therapy (Briolay et al., 2021).

The recent COVID-19 pandemic has revealed the effectiveness of lipid nanoparticles as mRNA vectors in the production of mRNA-based vaccines. Such vectors release the spike protein-coding mRNA into the body immune cells, promoting the production of COVID-19 spike protein and the consequent immune response by activating T-cells and the production of specific antibodies (Banerji et al., 2021).

As a consequence of the promising results of nanomedicine, we can expect a rapid spread and development of nanotechnology and new significant discoveries in the near future.

1.3 Nanoparticles and nanovectors in agriculture

As the application of nanotechnology in materials science and biomedicine has rapidly spread, the interest in its possible applications in agriculture raised considerably in the last decade towards the increasing need of a more sustainable agriculture to cover human food and vegetal-derived materials production and limit excessive tilling, abuse of pesticides and fertilizers in intensive cultivations which can lead to irreversible environmental damage such as eutrophication, land degradation and desertification (Slegers and Stroosnijder, 2008; Withers et al., 2014), influencing human lives and health of entire regions of the globe.

While the large-scale production and purification process (e.g. separation from the micro-emulsion in oil, water or other surfactants) of nanoparticles for medical and industrial use can be challenging and demanding in terms of resources and environmental impact (Royal Society (Great Britain) and Royal Academy of Engineering (Great Britain), 2004), eco-friendly, green production approaches can be used to synthetize nanoparticles starting from plant extracts (Alaa Y Ghidan et al., 2017), drastically limiting the impact of the production process and the release of potentially polluting and hazardous compounds in the environment (Huang et al., 2015).

As the scientific community is advancing studies on nanotechnology in agriculture, a large number of nanoparticles and applications have already been developed and are currently starting to spread as an integrating part of the so called “precision farming” to increase crop-yields while preserving the environment (A. Werner and J. Stafford, 2003). Magnetite (Fe_2O_3) nanoparticles have been reported to be effective in increasing plant germination and growth in *Solanum lycopersicum* (tomato) and its biomineralization (Shankramma et al., 2016), while CuO, FeO, AlO, MnO, NiO and ZnO NPs revealed effective in pest control as aphicidals (Ghidan et al., 2018), while silver have been proven to increase wheat growth and yield (Jhanzab et al., 2015). The synthesis of green-produced bio-nanoparticles of copper oxide (CuO), magnesium hydroxide (MgO), zinc oxide (ZnO) and magnesium oxide (MgO) was performed by extraction from *Punica granatum*, *Chamaemelum nobile* and *Olea europaea* and, upon foliar spray, proved to be effective in aphid pest control and antibacterial activity while no metal nanoparticle accumulation was recorded in the threated plants which, in some cases, also showed an improvement in growth and better fruits yield (Alaa Y. Ghidan et al., 2017).

In addition to their insecticidal and antimicrobial activity, other nanoparticles have been found to be effective fungicides, like nanosilver particles in the treatment of

Colletotrichum gloeosporioides phytopathogen (Madan et al., 2016) and nickel nanoparticles consistently inhibited mycelial growth of *Fusarium oxysporum* f. sp. *lactucae* and *Fusarium oxysporum* f. sp. *lycopersici* (Ahmed, 2016).

In addition to nanomedicine, nanoparticles have lately started to be considered as possible nanovectors for the release of RNA and other bioactive molecules into plant cells (Cunningham et al., 2018; Demirer et al., 2018).

DNA nanostructures have recently been used to deliver siRNA to silence target genes to confer disease and pest resistance. The role of the DNA nanovectors is to protect the siRNA from enzymatic degradation before passing through the cell wall and membrane and represent a valid alternative to transgenic modification of plants (Avellan et al., 2017).

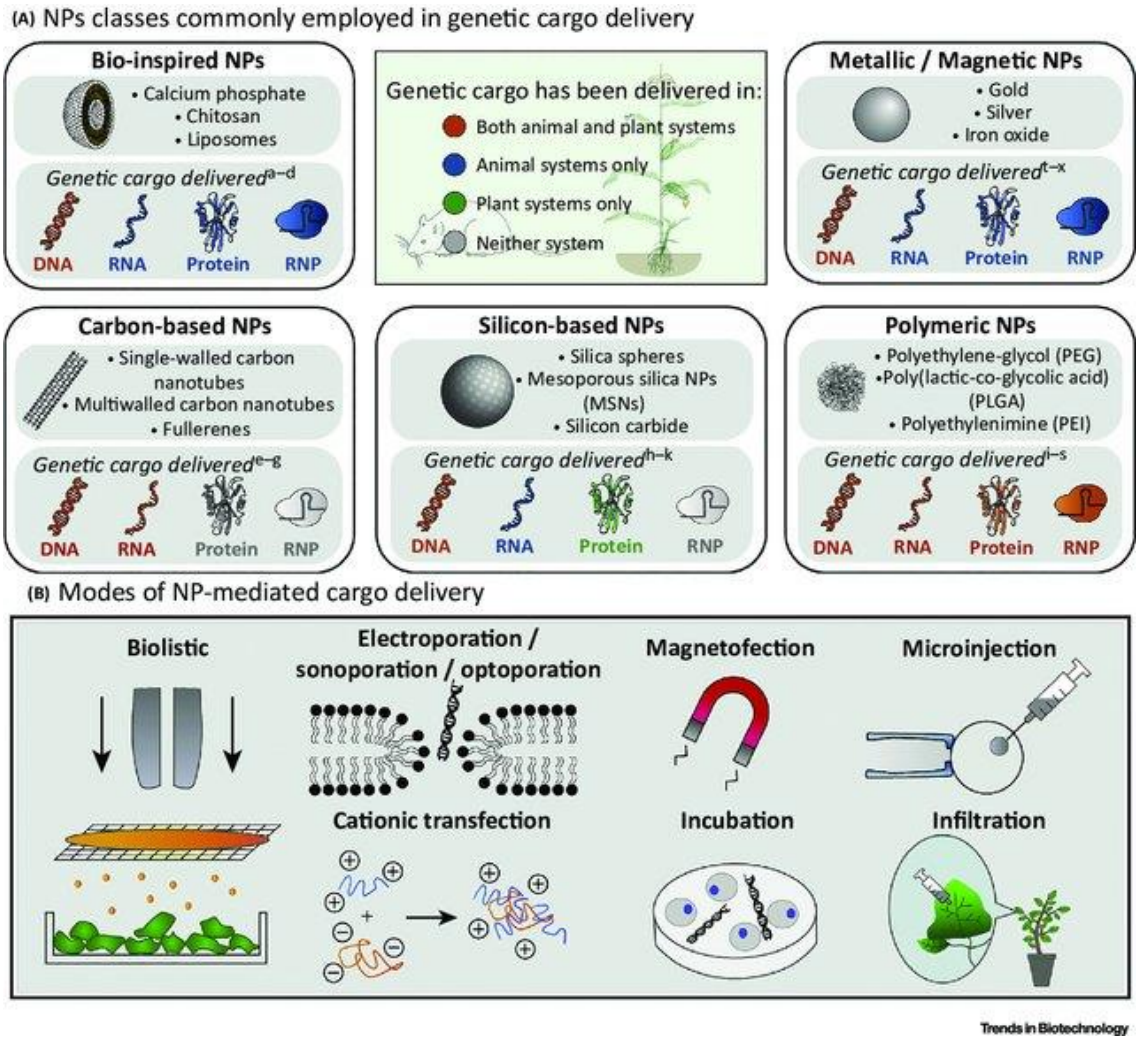

Figure 2. Types of nanoparticles used as genetic cargo deliverers (A) and bioactive molecules deliverers (B). Figure: Cunningham et al., 2018.

In addition, nanovectors have been successfully used to improve the uptake and efficacy of nanostructured (Mn, Fe, Cu, Mo, Zn) or traditional fertilizers (Liu and Lal, 2015) and a natural polymer such as chitosan have been used to produce NPs capable of controlled release of the N, P, K macronutrients (Aziz et al., 2016).

Besides the positive and encouraging results described so far, research also has to take into account the possible toxicity of NPs for plants. It has been reported that the accumulation in soil of some Fe, Cu, Zn, Si, Al, ZnO, TiO_2, Al_2O_3 and CeO_2 nanoparticles had detrimental effects on plants growth and useful soil bacteria, like *Pseudomonas putida KT2440* (Gajjar et al., 2009), fungi and invertebrates (Frenk et al., 2013; Waalewijn-Kool et al., 2013; Shen et al., 2015), making, in practice, their use unviable as an eco-friendly approach to agriculture. On the contrary, anti-pest nanovectors have high stability, solubility and enhanced uptake and proved to be very effective in the gradual release of their cargo (Duhan et al., 2017). As an example, organic or polymeric (e.g. poly(epsilon-caprolactone)) nanocapsules (NCs) and nanospheres (NSs) have been used as nanocarriers for herbicides like atrazine and triazines with very high biocompatibility (Tanaka et al., 2012; Grillo et al., 2015), demonstrating that polymeric nanoparticles represent the ideal candidates for cargo delivery in plants. The main advantage of this approach is the low production cost due to the use of naturally occurring biopolymers and their low environmental impact as a consequence of their biodegradability (Sampathkumar et al., 2020).

1.4 Lignin nanovectors

1.4.1 Lignin origin and structure

In the context of circular and green economy, the use of lignin as a natural, biodegradable, polymer for the fabrication of nanoparticles and nanovectors represent a promising approach towards sustainable agriculture (Soppimath et al., 2001).

Lignin is a natural, low-cost and sustainable by-product of pulp and paper industrial processing and constitutes the second most abundant biopolymer available on Earth after cellulose. Lignin is deposited in the secondary wall of plants and is the fundamental polymeric constituent of water and minerals transporting structures in

plants (xylem), as well as providing mechanical resistance (sclerenchyma) and protection from abiotic and biotic aggressions (lignified cell walls).

The chemical structure of lignin is represented by a combination of different acids and phenylpropyl alcohols (p-coumaric, coniferyl and sinapyl alcohol) assembled into a three-dimensional, highly branched and aromatic rings-rich, amorph structure with a multitude of different functional groups (carbonyl, methoxy, aliphatic, phenyl and phenolic groups, etc.) and a high molecular weight. The fraction of each phenylpropyl alcohol in the polymer is variable depending on the tissue, the plant group and the species. Lignin is insoluble in acids, but soluble in alkali solutions and organic solvents (Dastpak et al., 2020).

Many types of lignin, with variable properties, can also be obtained by different industrial production processes such as kraft lignin, lignosulfonate, organosolv lignin and soda lignin (Tang et al., 2020).

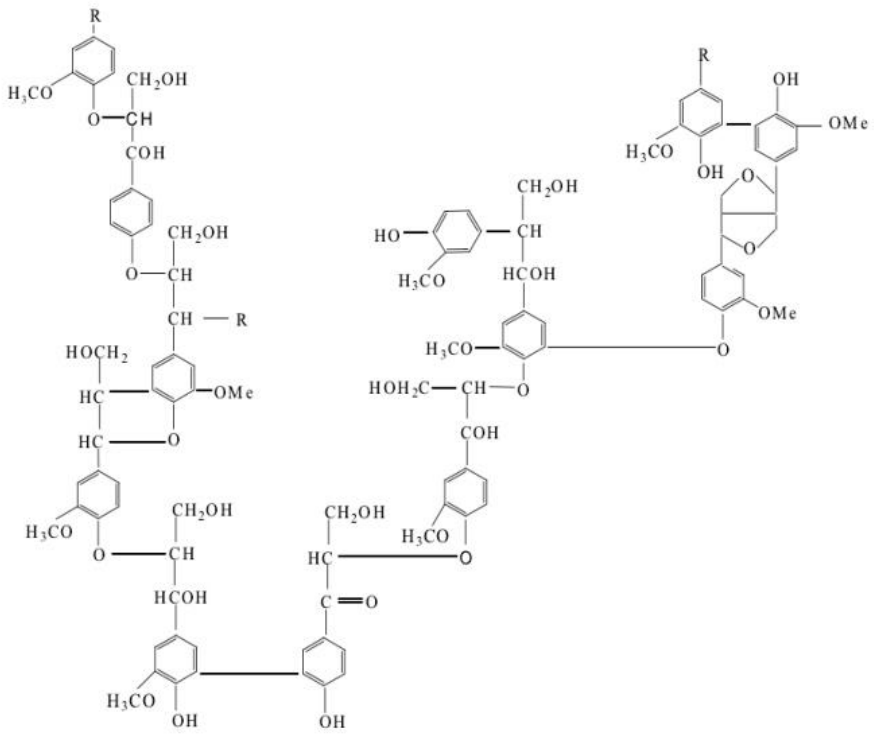

Figure 3. A possible structure of lignin molecule. Picture by Tang et al., 2020.

1.4.2 Production of lignin-based nanoparticles

The minimal cost, abundancy, biocompatibility and its unique antioxidant, antimicrobial, emulsifying and UV-blocking properties (Agustin et al., 2019) make lignin a suitable candidate for the production of high-value added industrial products as well as

nanomaterials with the most diverse applications (Tang et al., 2020). Lignin-based nanoparticles and nanocapsules (NCs) have been obtained by different procedures, the choice of which is dependent on their final application. Lignin nanoparticles have been successfully prepared by acidic precipitation and successive ultrasonication by (Agustin et al., 2019) and (Gupta et al., 2014). Lignin colloidal spheres have been assembled starting from pulping spent liquor by self-assembly method by Qian et al., 2014 and by solvent exchange method by dissolving kraft lignin into tetrahydrofuran (THF) and subsequently using dialysis bags immersed in excess water, resulting in very stable nanoparticles in water with adjustable size as a function of the starting lignin concentration (Lievonen et al., 2016). Ultrasonication for 60 minutes and successive drying of a lignin solution resulted in particles of variable size, ranging from 10 to 50 nanometres (Gilca et al., 2015). Additional methods include cross-linking (Yiamsawas et al., 2014) and by using CO_2 in a supercritical antisolvent process starting from an acetone/lignin solution (Lu et al., 2012).

1.4.3 Applications of lignin nanoparticles

The scientific community has only recently started to consider lignin as a valid material for the fabrication of nanoparticles (Sipponen et al., 2019). Its low cytotoxicity and the possibility of incorporating otherwise cytotoxic or unsoluble biomolecules, as well as their biocompatibility, represent valuable properties which open up a multitude of possible applications in both bionanomedicine and agriculture.

Colloidal nanospheres obtained with different processes have already shown consistent results in encapsulating and releasing drugs like ibuprofen (Li et al., 2017) and resveratrol as an anti-cancer treatment (Dai et al., 2017) or for controlled release of pesticides like avermectin (Deng et al., 2016; Zikeli et al., 2019).

Lignin reverse colloidal spheres have revealed to be very effective in sunscreen creams thanks to their UV absorbance (Qian et al., 2017). In addition, thanks to the presence of methoxy and phenolic hydroxyl groups, lignin nanoparticles can be used, pure or as an additive into materials, to engineer various materials with antioxidant properties (Tian et al., 2017; Yang et al., 2016).

Despite many studies have already confirmed the potential of lignin nanoparticles in many applications, the use of lignin nanovectors as carriers of active biomolecules in plants has still to be investigated in detail (Pérez-de-Luque, 2017). The possibility of loading a cargo in hollow-structured lignin nanocapsules and the mobilization of these

particles suggest a possible employment in the delivery of biomolecules in plant tissues. To fulfill this task, many aspects need to be taken into account when engineering such nanovectors. The uptake of extraneous particles from plant roots or leaves involves complex processes and depends on the properties of the nanoparticle itself, its interaction with the environment, the dispersion method, the composition of the suspension solution and the species-specific physiology of the target plant. In addition, once internalized by the plant, the movement of the particles can occur by two ways: apoplastic (outside the plasma membrane) and/or symplastic (through cell membranes, by clathrin or caveolin mediated endocytosis), implying peculiar physiological and morphological events which need to be considered when designing a new nanovector and are still partially known (Pérez-de-Luque, 2017). Figure 4 shows the possible uptake routes and movements of nanoparticles in plants.

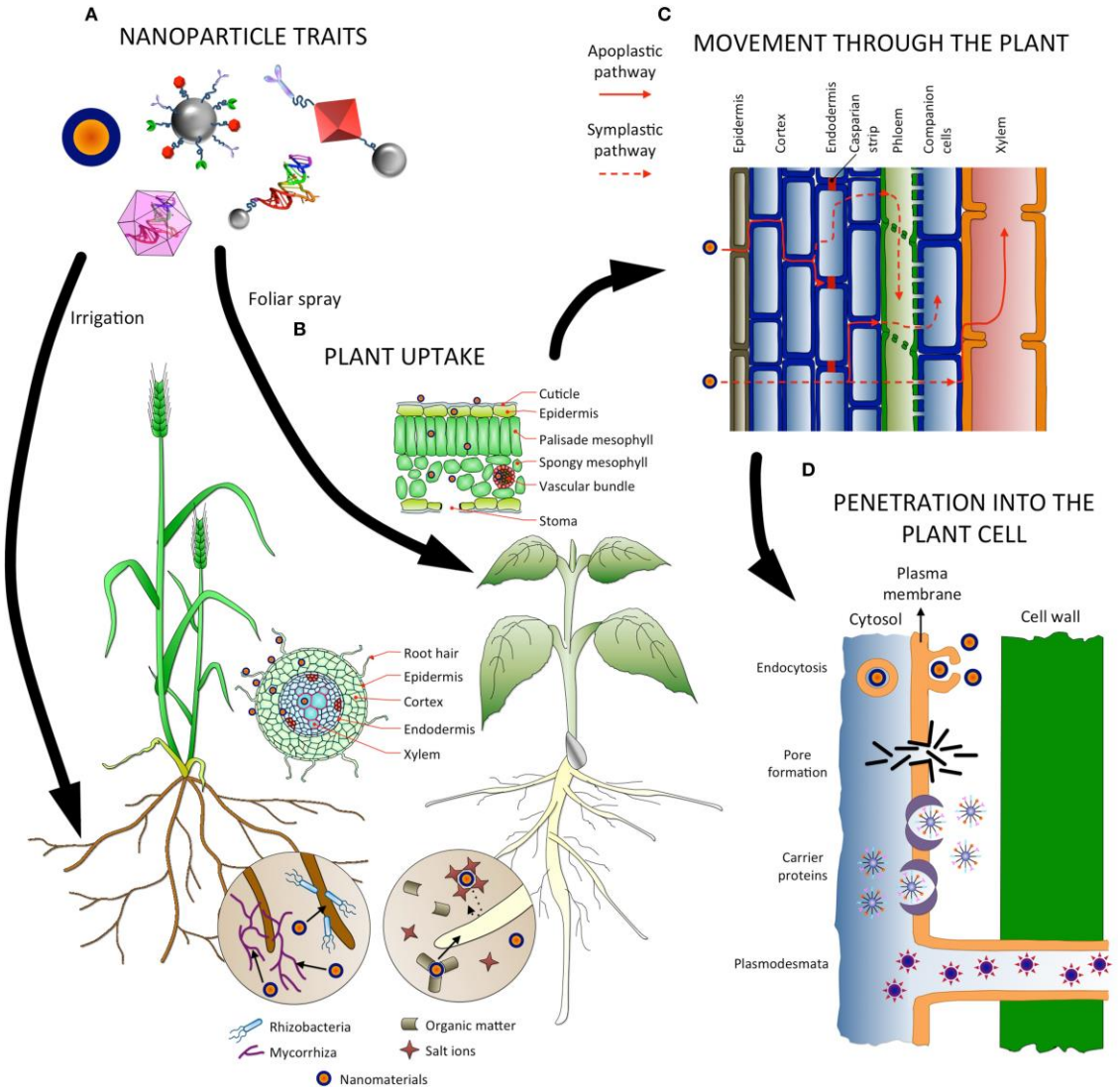

Figure 4. Various nanoparticles (A), their possible uptake pathways (B), apoplastic and symplastic movement (C) and penetration modalities into plant cells (D) are shown. Figure from Pérez-de-Luque, 2017.

Although challenging, the development of lignin nanovectors could yield many beneficial outcomes in sight of a more sustainable agriculture and circular economy. As a consequence, further efforts should be directed towards the study of lignin nanoparticles, their uptake modalities and their employment as cargo-deliverers in plants.

2. Hypothesis and aims

The purpose of the present work is to investigate the uptake modalities of lignin nanocapsules (LNCs) produced according to Falsini et al., 2019 and ascertain their possible application as sustainable nanovectors of bioactive molecules such as antibiotics, antimicotics or hormones in agriculture. Hence, several experiments, ranging from the administration of different dilutions of the LNCs solution, exposure time and administration modalities have been carried out on seedlings of *Eruca sativa* (Mill.), *Eragrostis tef* (Zucc.) and *Arabidopsis thaliana* (L.). Previous preliminary studies on the interaction of these LNCs with young seedlings (Falsini et al., 2020, 2019) revealed the presence of the particles in roots and stems, but the modalities of their uptake and mobilization in plant tissues have not been investigated yet. The main hypothesis comprises a possible uptake route by the entrance through roots hair and roots epidermis, with a subsequent apoplastic and/or symplastic movement towards the Casparian strip. In addition, in order to reach the xylem vessels and successively be translocated to the upper regions of the plant, the particles require to cross the Casparian strip through the symplastic way. To allow their localization and visualization, the LNCs have been loaded with Fluorol Yellow 088 (Sigma-Aldrich) fluorescent dye during the production process in order to be located in plant tissues by fluorescence microscopy. For the imaging, different techniques involving both optical and electron microscopy have been chosen. Considering that the research and employment of nanoparticles as nanovectors in agriculture is still at its dawn, the experiments conducted in this study aim to verify the above hypothesis and to contribute to the development of nanotechnologies for improving agriculture productivity and sustainability.

3. Materials and methods

3.1 Plants choice and seedlings incubation

Eruca sativa and *Eragrostis tef* have been chosen for the experiments for their wide consumption as food and *Arabidopsis thaliana* for its role as model-plant in research. In addition, the chosen plants are representative of both monocotyledons (*Eragrostis tef*) and dicotyledons (*Eruca sativa, Arabidopsis thaliana*).
Seeds of *Eragrostis tef* and *Eruca sativa* were placed on filter paper in petri dishes, kept moist in tap water and incubated in an incubation chamber at 26 °C with 14 hours photoperiod in the Biomorphologies laboratory of the Department of Biology of the University of Florence, while *Arabidopsis thaliana* seedlings were cultivated on Linsmaier and Skoog (LS) medium, pH 5.7, with the addition of 1% agar at the Department of "Ortoflorofrutticoltura" of the University of Florence under similar conditions.

3.2 Preparation of lignin NCs

3.2.1 Production by ultrasonication

Different types of lignin NCs have been prepared by ultrasonication for the experiments:

1) 1% lignin empty NCs (ENCs);
2) 5% lignin empty NCs;
3) 1% lignin NCs loaded with Fluorol Yellow 088 (FY088) from Sigma-Aldrich (FNCs);
4) 5% lignin NCs loaded with Fluorol Yellow 088 from Sigma-Aldrich (FNCs);

Each one of these emulsions was prepared by mixing kraft lignin (Sigma-Aldrich) and the oil/acetone/FY088 emulsions in both pH 13.5 and pH 11.7 alkali solutions, obtained by dissolving KOH in milli-Q water, resulting in a total of eight different types of NCs emulsions. Two different alkali solutions were chosen as lignin solubility in water increases with pH.

FNCs were prepared by dissolving one part of an acetone/olive oil 1:1 v/v emulsion in ten parts of the alkali solution (pH 13.5 or pH 11.7, 1% or 5% lignin). FY088 was dissolved in the olive oil at 0.1% w/v concentration beforehand as a fluorescent marker. FY088 ($C_{22}H_{16}O$, mw 296.36) is an effective lipids fluorescent dye with an absorption/emission of 450/515nm which allows the localization of the FNCs in plant tissues under fluorescence microscopy.

Emulsions for obtaining ENCs were prepared without the addition of FY088 to the oil.

The resulting eight emulsions were sonicated by a Branson 450 Digital Sonifier set at 50% power (200W) for 15 minutes at 1s on/2s off cycles to avoid overheating (Figure 5).

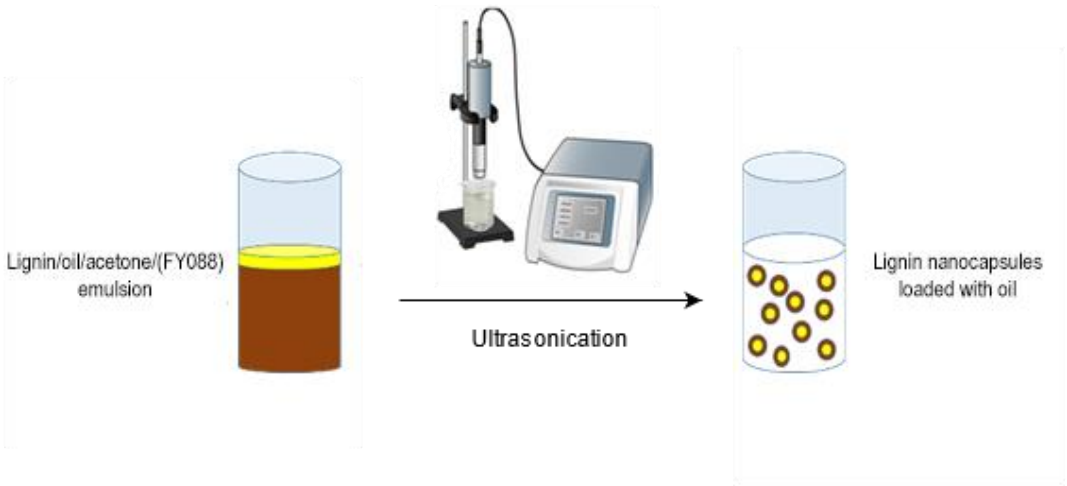

Figure 5. Lignin nanocapsules production. The lignin/oil/acetone/FY088 emulsion is ultrasonicated to obtain lignin hollow structures containing oil marked with the fluorescent dye FY088.

The size of the particles was characterized by Dynamic Light Scattering (DLS) on a Malvern Zetasizer Nano ZS (Malvern Instruments Southborough, USA) using a 4mW He-Ne 633nm laser with backscattering detection. The size distribution resulted in the range between about 100-800nm with a peak 232nm and a polydispersity index (PDI) of 0.251 for the 1% lignin emulsion and a peak of 305nm for the 5% lignin emulsion. Results of the analysis are reported in Figure 6.

.

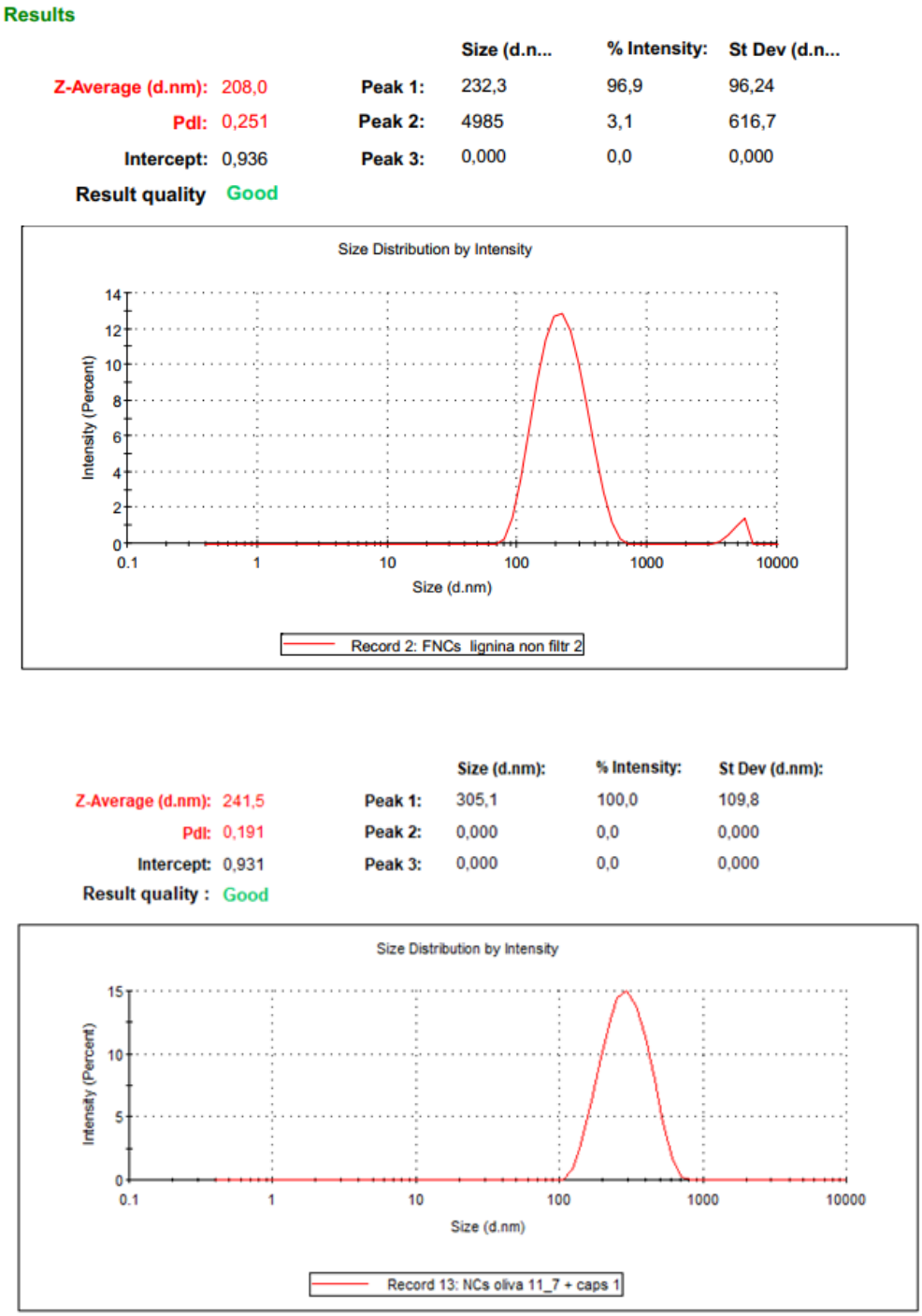

Figure 6. Dynamic Light Scattering of 1% w/v lignin (above) and 5% w/v lignin (below) of nanocapsules loaded with Fluorol Yellow088 obtained by ultrasonication.

The final pH of all NCs emulsions settled around neutral values and they have been stored in vials in a refrigerator at 4 °C after their production.

The so obtained NCs were then administered to the seedlings in different modalities and dilutions during the experiments (e.g. 1:5, 1:100 v/v in dH_2O).

3.2.2 Filtration of NCs obtained by ultrasonication

The 1:100 v/v dilution of 1% w/v lignin FNCs obtained by ultrasonication was filtered first through 0.45µm syringe filter and successively through a 0.20µm syringe filter to discard the bigger sized FNCs. The DLS results after filtration through 0.20µm filter are shown in Figure 7, showing a peak diameter of 125nm and a PDI of about 0.2.

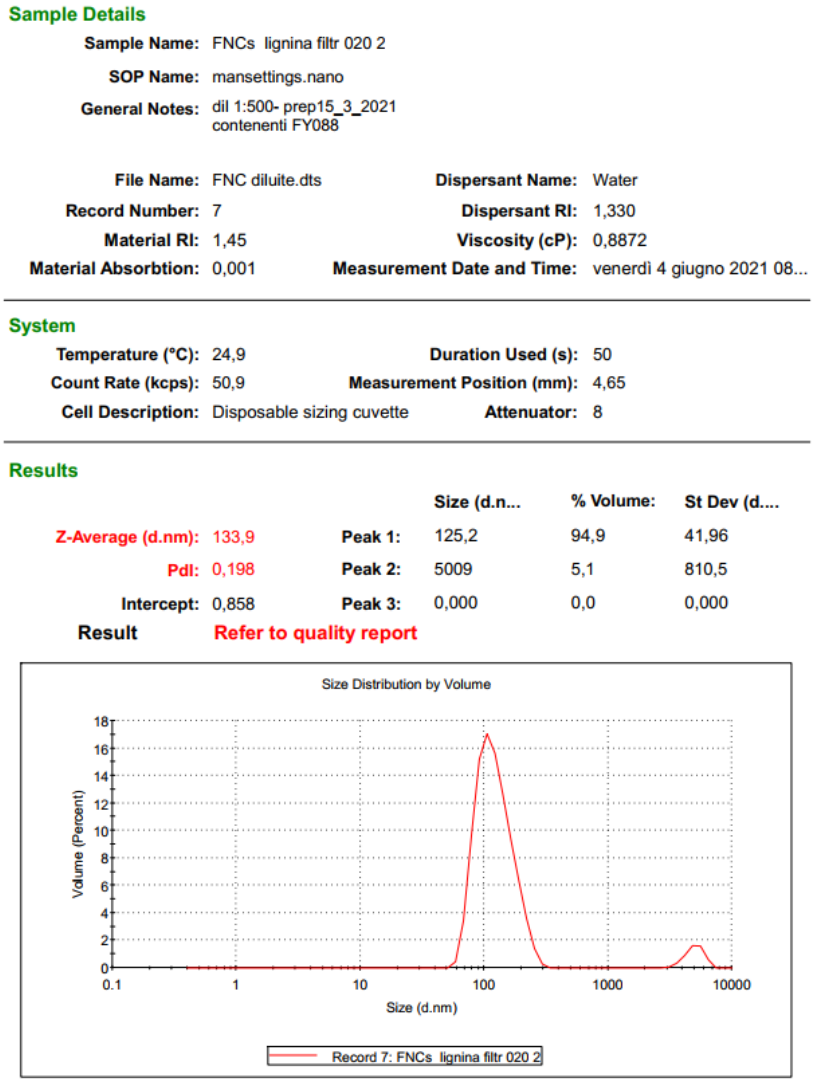

Figure 7. Dynamic Light Scattering of 1:100 v/v dilution of 1% lignin FNCs after sieving through a 0.45µm and successively a 0.20µm syringe filter.

3.2.3 Production by extrusion

In addition, the NC obtained as described in 3.2.2, were also processed by an extrusion device (Figure 8) through 50nm membranes to further reduce their size. The solution was passed through the device membrane several times and the DLS showed that the size distribution has a skew shape, with a large component below 100nm, with a peak diameter of 146.4nm (Figure 9). However, the measured diameter expanded up to about 300nm, indicating that extensive size reduction is difficult, probably due to the restraints imposed by spontaneous curvature and by the self-assembly requirements themselves.

Figure 8. Example of extruder similar to the one used for the experiment.

Sample Details

Sample Name:	FNCs estruse 2		
SOP Name:	mansettings.nano		
General Notes:	campioni 1:5 filtrate 0.2 micron e poi estruse (200 - 50 nm)		
File Name:	NCs fluorocromo 30-6-...	**Dispersant Name:**	Water
Record Number:	10	**Dispersant RI:**	1.330
Material RI:	1.45	**Viscosity (cP):**	0.8872
Material Absorbtion:	0.001	**Measurement Date and Time:**	mercoledì 30 giugno 202...

System

Temperature (°C):	25.1	**Duration Used (s):**	50
Count Rate (kcps):	201.2	**Measurement Position (mm):**	4.65
Cell Description:	Disposable sizing cuvette	**Attenuator:**	9

Results

			Size (d.n...	% Volume:	St Dev (d.n...
Z-Average (d.nm):	141.0	**Peak 1:**	146.4	96.3	111.8
PdI:	0.222	**Peak 2:**	4126	3.7	1070
Intercept:	0.960	**Peak 3:**	0.000	0.0	0.000
Result quality	Good				

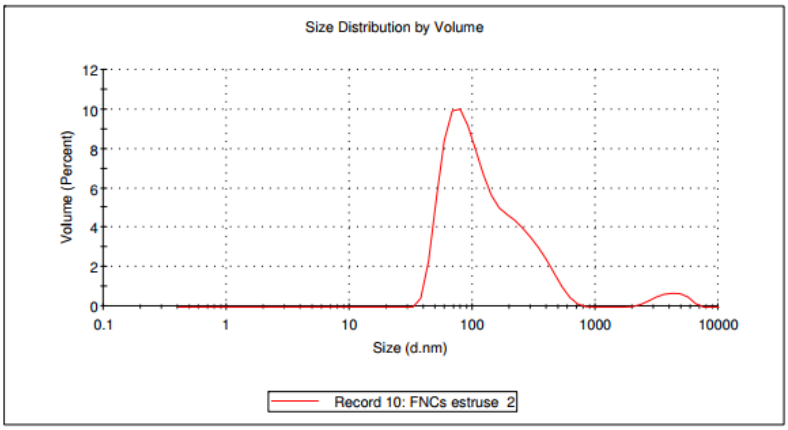

Figure 9. Dynamic Light Scattering results after extrusion through 50nm pores membrane.

3.3 Fluorescence microscopy

Fluorescence microscopy is a valuable imaging tool which is the ideal choice for localizing the NCs loaded with a fluorescent marker used in this study. A Leitz DMRB fluorescence microscope equipped with a Nikon DS-5M digital camera using 460nm excitation light and an emission filter 530/30 to briefly screen the FNCs in samples by conventional widefield fluorescence. In addition, different fluorescence microscopy techniques have been used depending on instrument availability and investigation purpose. All of the reported images are raw images with no software modifications or

enhancements and annotations and montages have been done with Fiji (https://imagej.net).

3.3.1 Light sheet fluorescence microscopy (LSFM)

Light sheet fluorescence microscopy offers the possibility of imaging large volumes of relatively transparent samples by illuminating them with a thin sheet of excitation light projected by an illumination objective, while collecting the fluorescence emission with a detection objective. In this study, a custom-made confocal light sheet microscope located in the European Laboratory for Non-Linear Spectroscopy of the University of Florence, Italy, was used to obtain 3D data of seedlings exposed to the FNCs. The system (Figure 10) is equipped with multiple wavelength excitation lasers (530nm laser was used for the experiments), two opposite illumination arms equipped with Nikon 10x/0.3 objectives for isotropic illumination of the sample, thus limiting artifacts derived by anisotropic illumination, an Olympus 10x/0.6 multi-immersion detection objective and a Hamamatsu Orca Flash 4.0 camera for the recording of data. The pixel size of the image is 0.65μm and the z-step is 2μm. The excitation light sheet is scanned onto the sample by galvanometric scanners. The illumination and detection objectives are placed in a sample chamber filled with immersion liquid with a refractive index (RI) matched with the refractive index of the quartz cuvettes (1.54) where the samples are placed for the imaging. Matching the RI is fundamental for limiting the spherical aberrations derived by an eventual mismatch. In such a setup, seedlings were imaged *in vivo*, immersed in tap water inside the quartz cuvette. The system allowed to record large 3D volumes of the roots of the samples.

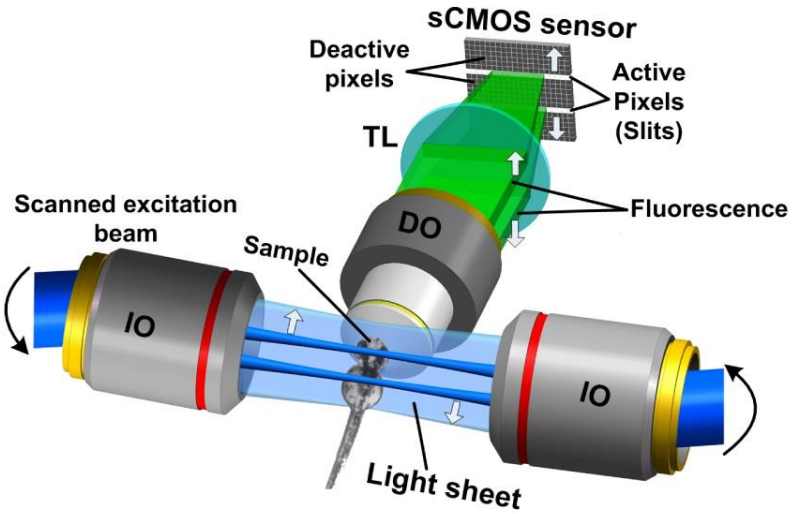

Figure 10. Scheme of the scanning light sheet microscope used for the imaging. The illumination light sheet is scanned through two illumination objectives (IO) and the fluorescence is captured by a detection objective (DO) and the final image is recorded by the camera sensor. Image from (Yang et al., 2015).

3.3.2 Confocal laser scanning microscopy

Confocal laser scanning microscopy (CLSM) is a point scanning microscopy technique which provides optical sectioning imaging by excluding the out-of-focus blur thanks to two confocal pinholes of variable size placed on a conjugate image plane in the illumination path and in the detection path. As a result, the Airy disks in the PSF are cut off and the lateral resolution is increased depending on pinhole size up to about 30% the resolution of a standard widefield microscope and can be approximated to:

$$R_l = \frac{0.4\lambda}{NA}$$

In addition, the PSF is also stretched in the axial direction, resulting in an increased axial resolution and optical sectioning capability of the system and can be described by the approximation:

$$R_a = \frac{1.4\lambda\eta}{NA^2}$$

Where η is the refractive index of the medium. Photomultipliers (PMTs) are used to collect and amplify the emission light signal during the raster scanning of the sample, converting it into an electron signal which is used to build the final image by a software. ("Confocal Microscopy - Resolution and Contrast in Confocal Microscopy | Olympus LS," n.d.).

In this study a Leica TCS SP5 confocal microscope was chosen for its high resolution and optical sectioning capability, allowing to image as deep as about half the thickness of a seedling root, depending on species. The imaging was performed with a Leica 40x/1.25 HCX PL APO CS oil UV objective and a pinhole size corresponding to 67.9μm. The excitation wavelength for the FY088-loaded NCs was 458nm and the emission peak was calculated by a lambda scan and corresponded to 510nm, slightly diverging from the 515nm reported by the manufacturer, probably as a result of the chemical surroundings. The 5nm resolution of the detection system allowed to easily distinguish the signal from the FNCs from the cell walls autofluorescence (530-550nm).

For propidium iodide (PI, Signma Aldrich) experiments, the 514nm excitation laser set at 20% power was used and emission was recorded at 615nm peak.

3D volumes of samples were acquired with a z-step corresponding to 0.5μm.

3.3.2 Two-photon excitation fluorescence microscopy (2PEFM)

Two-photon excitation microscopy, is a fluorescence point scanning technique which excites a fluorophore by using two photons carrying approximately half the energy (double wavelength) necessary to excite the electron of that fluorophore from its ground state to an excited state. In order for this event to occur in one quantum event, the two excitation photons need to reach the molecule within one femtosecond time frame. Upon relaxation of the excited electrons back to their ground state, a photon of higher energy than either of the excitation photons is released, corresponding to the emission wavelength of the fluorophore. To achieve this, high power Ti:Sa infrared (~800-1040nm) pulsed femtosecond lasers (80Mhz pulses, up to 150MW peak power) need to be used. Since the probability for simultaneous absorption of two excitation photons is very low, the excitation events only occur within a small volume (about one femtoliter) at the focal spot of the objective lens, where the photon density is the highest (Figure 11). As a consequence, the resulting PSF is stretched both laterally and axially compared to a

conventional widefield microscope, resulting in higher lateral resolution and an optical sectioning equivalent to CLSM (“Advanced Applications,” n.d.; Mostany et al., 2015).

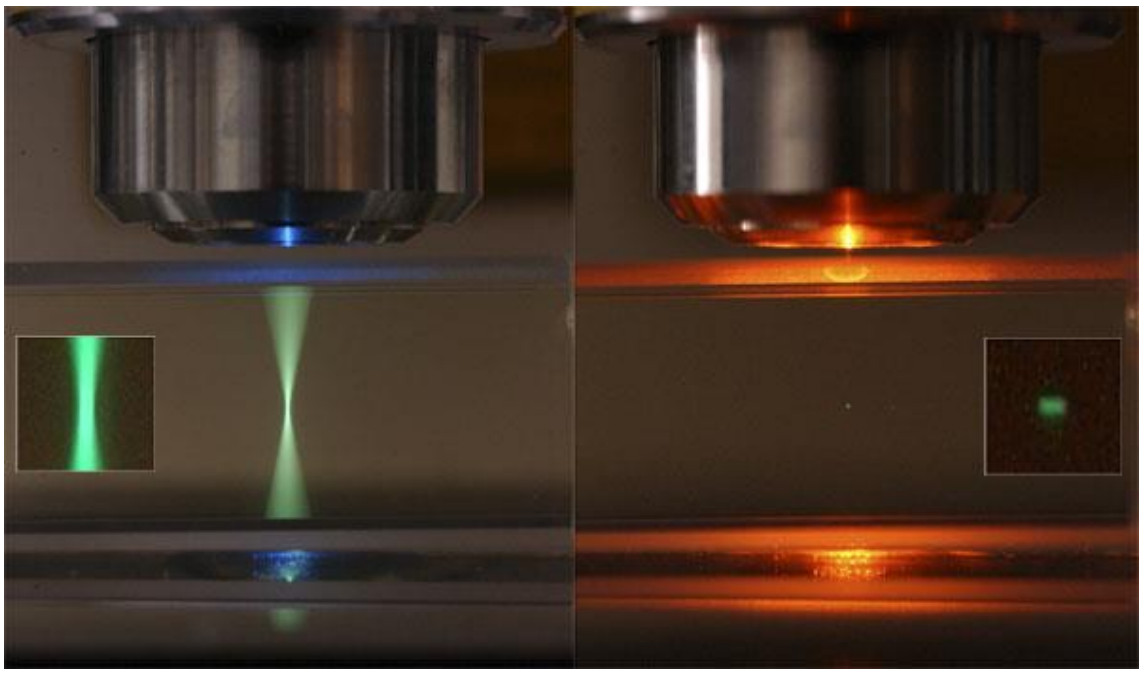

Figure 11. Single photon (left) and two-photon (right) excitation comparison. In 2PEFM excitation (and thus fluorescence) only occurs in a small volume at the focal spot of the objective, while in conventional single photon microscopy, excitation occurs along the whole cone of excitation light resulting in higher photobleaching and photodamage. Image by Steve Ruzin and Holly Aaron, UC Berkeley (https://microscopy.berkeley.edu).

The main advantage of 2PEFM resides in its capacity to image as deep as 1 millimeter into a relatively transparent tissue, due to the reduced scattering and increased penetration of infrared wavelengths compared to the shorter wavelengths used in conventional microscopy. A second advantage is the low photobleaching and phototoxicity, making this technique well suited for *in vivo* imaging. A possible disadvantage can be the heating of the sample due to the high laser power and the high absorption of infrared light by water (Giguère and Harvey, 1956).

For the experiments, a custom-made 2PEF microscope located in the European Laboratory for Non-Linear Spectroscopy of the University of Florence, Italy, was used to localize the FNCs and obtain 3D high resolution datasets of the seedlings *in vivo*. This instrument was chosen for its high resolution and allowed to image up to 180µm deep into the plant tissues. Deeper imaging was not possible due to the scattering caused by the cell walls and cytoplasm content in uncleared living samples. The excitation wavelength of the Ti:Sa laser was set to 900nm and a 520/30nm emission filter was used to selectively record the signal from the FNCs. 3D volumes with a z-step of 2µm and

pixel size of 440 nm were recorded using a Zeiss plan-apochromat 20x/1.0 water dipping microscope objective. Despite autofluorescence from cell walls was also emitting in the same wavelength range, its signal was a lot lower than the quantum yield of the fluorophore, resulting in a high signal-to-background ratio of the FNCs in the images.

3.4 Transmission electron microscopy (TEM)

Transmission electron microscopy provides high magnification and high resolution images of the ultrastructure of the sample by letting a beam of accelerated electrons through thin sections (<100 nm) instead of light. Thanks to their very low wavelength, the resolution of a conventional transmission electron microscope can be as low as 0.1 nm (1 Å). The wavelength of an electron, without considering the deterministic effects, can be described by:

$$\lambda = \frac{h}{\sqrt{2meV}}$$

Where h is the Planck's constant, m the mass of the electron, e the charge of the electron and V the accelerating voltage. Considering this, Abbe's equation for resolution can be reformulated for an electron microscope as:

$$d = \frac{0.753}{a\sqrt{V}}$$

Where a is the half aperture angle and V is the accelerating voltage ("Introduction to Electron Microscopy - Advanced Microscopy - Imaging Facilities - The University of Utah," n.d.; "MICROSCOPY TECHNIQUES | Electron Microscopy - ScienceDirect," n.d.).

In this study, a Philips EM201 TEM was used to localize the NCs in plant roots cells and to visualize their ultrastructure and the eventual structural modifications at the cell wall and plasma membrane level as a consequence of particle internalization.

3.5 Sample preparation for microscopy

3.5.1 Sample preparation for optical microscopy

For fluorescence widefield microscopy, seedlings roots, stems and leaves have been cut in small pieces about 3-4mm long, put on a microscope slide with tap water as mounting medium to avoid osmotic stress and plasmolysis and covered with a coverslip before observation (Figure 12).

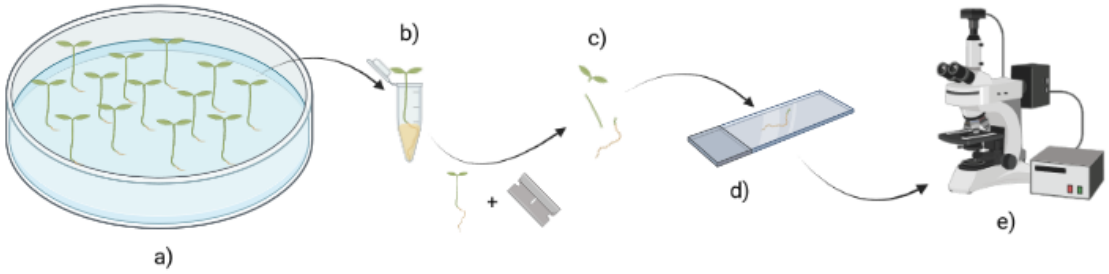

Figure 12. Sample preparation for fluorescence microscopy. Seedlings grown in petri dishes (a) were put in contact with the FNCs emulsion (b). After the administration time, seedlings were cut with a disposable razor blades into small pieces (c), put on a microscope slide (d) and observed with a Leitz DMRB fluorescence microscope.

Two-photon microscopy, equipped with a water dipping objective, allowed *in vivo* imaging of the seedlings immersed in tap water as medium. Seedlings were placed as straight as possible on petri dishes containing a layer of black silicone on which the small plants were secure by the mean of small pins as shown in Figure 13.

Figure 13. Sample preparation for 2PEFM. Seedlings were kept in position on a petri dish containing a silicone layer by metal pins.

For LSFM, seedlings were put in a quartz cuvette of 10x10 mm section, immersed in tap water for *in vivo imaging*. The cuvette was placed in the imaging chamber, surrounded by the imaging medium having RI matched with quartz RI (Figure 14).

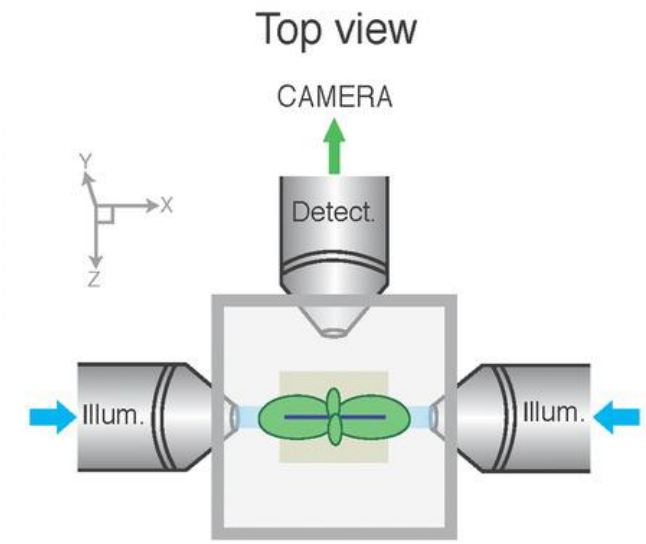

Figure 14. Light sheet microscopy sample placement. Seedlings in the quartz cuvette were illuminated isotropically by the two illumination objectives and the fluorescent signal was captured by the detection objective. Image from (Berthet and Maizel, 2016).

For CLSM, whole seedlings were placed on a microscope slide and covered with a large coverslip, mounted in Linsmaier and Skoog 1:1 v/v in water, for *in vivo* imaging.
All seedlings, prior to imaging, have been washed two times in the same solution used for mounting in order to remove excess FNCs adhering to roots hair, epidermis and mucilage.

3.5.2 Sample preparation for TEM

Samples (roots) to be observed by TEM have been cut in 3-4 mm long pieces from living seedlings and fixed in PBS 0.1M pH 7.2 with 2.5% glutaraldehyde, washed in PBS and post fixed in osmium tetroxide 1% in PBS for 1.5 hours to enhance the contrast of membranes. After fixation in osmium, the samples have been washed twice in PBS for 10' before dehydration in alcohol series (30%, 40%, 50%, 60%, 70%, 80%, 95% v/v and absolute alcohol two times) 10' in each solution. The choice of many slightly increasing alcohol concentration was done to better preserve the ultrastructure of the samples. After the last absolute alcohol step, the samples have been immersed two times in propylene oxide, 10' each. Spurr resin (Electron Microscopy Sciences©) was used as embedding

medium for the samples. Resin components have been mixed together and put in a vacuum chamber to remove air prior to sample embedding. Afterwards, the samples have been transferred from the propylene oxide solution to 50%, 70%, 100% v/v propylene/resin in 60' steps before polymerization in embedding molds at 70 °C for 9 hours.

After polymerization, the blocks containing the samples were trimmed with a razor blade to expose the sample for the cut. Thin sections of about 70 nm thickness were cut with a Reichert ultramicrotome and placed on TEM grids. Sections on grids were put on 3% w/v lead citrate drops for 10' and successively stained on 1% w/v potassium permanganate in PBS to enhance lignin contrast as suggested by Reza et al., 2015.

4. Results

Despite nanotechnology has already found many applications in agriculture (A. Werner and J. Stafford, 2003), the development of efficient nanovectors to deliver bioactive molecules to plants is still at its dawn and could represent a new frontier towards sustainable agriculture.

The present study aimed to localize the FNCs, prepared as previously described in (3.2), in plant tissues and eventually identify their uptake and transport routes into plant vascular bundles to evaluate their viability as nanovectors. For the task, several experiments were carried out by administering the FNCs prepared in different dilutions and filtrations as reported in (3.2). Multiple imaging techniques were used to locate the FNCs, depending on the availability of the instrument and on the purpose of the experiment. Most of the imaging was performed in the transition zone, above the root apex, where endocytosis and uptake are more active.

4.1 Preliminary experiment on emulsions toxicity

A preliminary experiment was necessary to evaluate the reaction of *Eragrostis tef* seedlings upon administration of the four NCs emulsions produced in pH 13.5 solution: empty NCs (ENCs) and Fluorol Yellow088 loaded NCs (FNCs), with both 1% or 5% lignin content for a total of four. *Eragrostis tef* seedlings which have been incubated for

a week were placed into a volume of 150µl of each emulsion in a petri dish for a total of three plants for each of the four emulsions. In addition, three seedlings were placed in the same tap water they have been incubated with as a control (Figure 15). Afterwards the plants were incubated in the same germination chamber for 24 hours before analysis by fluorescence microscopy.

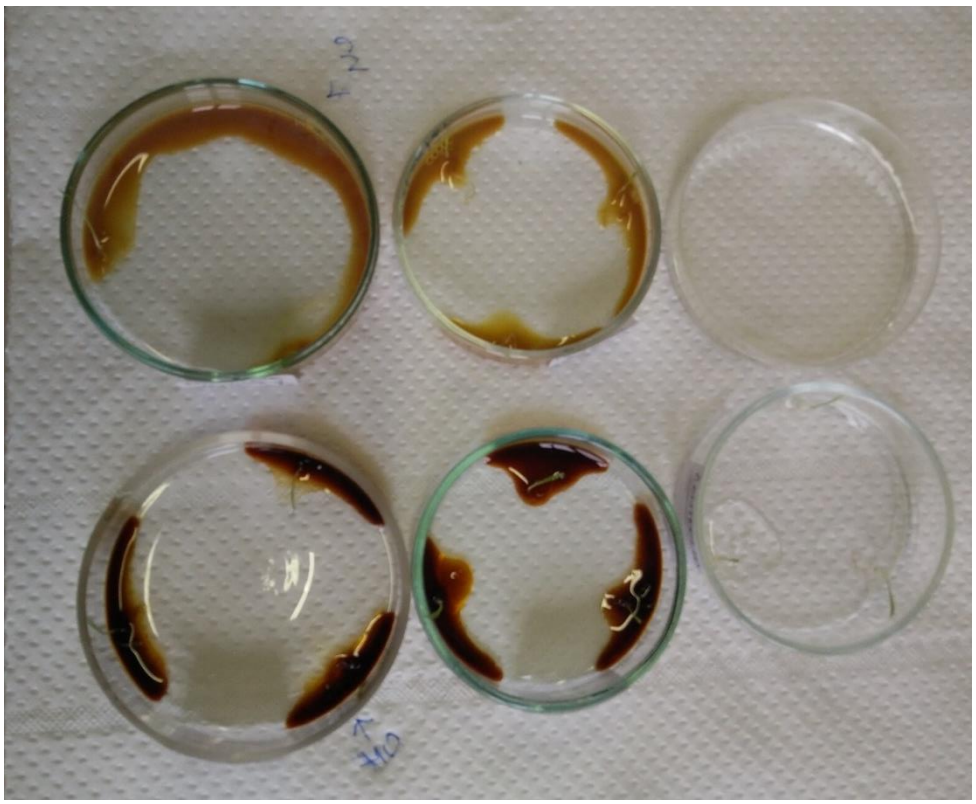

Figure 15. Seedlings were placed in contact with the four different formulations of pH 13.5 lignin NCs and incubated for 24 hours.

After one day of incubation, most of the plants in contact with the NCs emulsions showed evidence of death, while the control did not. The roots, stems and leaves of plants exposed to NCs showing less evidence of damage, were washed in tap water to remove the excess emulsion and inspected by widefield fluorescence microscopy which revealed no evidence of the presence of FNCs inside root cells.

A second experiment was carried out by exposing *Eruca sativa* 9 days old seedlings to each one of the emulsions described in (3.2), thus including NCs produced in both pH 13.5 and pH 11.7 solutions. Each emulsion has been diluted 1:5 v/v in dH_2O before administration. Two seedlings have been put in an Eppendorf vial containing 300µl of each emulsion and incubated for 24 hours. After the incubation period, all plants exposed to pH 13.5 NCs emulsions resulted dead, while those exposed to pH 11.7 emulsions were

lively and were observed under fluorescence microscopy which revealed the presence of FNCs in plants exposed to both 1% and 5% lignin content emulsions.
As a consequence of these results, emulsions of NCs produced in pH 13.5 solution were discarded for the following experiments. The 5% lignin emulsion was also discarded for the presence of abundant undissolved lignin and for the bigger average size of the particles (Figure 6).

4.2 Preliminary imaging by LSM and 2PEFM

4.2.1 Light-sheet microscopy

Light-sheet microscopy has been chosen to visualize FNCs in a two weeks old *Eruca sativa* seedling root after 24 hours administration of 1% lignin pH 11.7 FNCs emulsion diluted 1:5 in dH_2O. The experiments were carried on at the European Laboratory for Non-Linear Spectroscopy of the University of Florence.
Light sheet microscopy was chosen for its ability to acquire a large 3D volume of the sample *in vivo* to have an overview of the whole root, including its surrounding hair. The seedlings have been placed in Eppendorf vials containing the FNCs emulsion as shown in Figure 12b for 24 hours, washed and mounted in the quartz sample chamber for the imaging. The recorded images showed the presence of FNCs clusters probably adhering to the root hair and to the epidermis of the root as can be seen in Figure 16 and Figure 17, but no evidence of internalization of FNCs in both hair and roots cells was observed due to the severe scattering probably as a consequence of the presence of the cell wall and artifacts produced by the shadowing from external hair. These detrimental effects denied the possibility of correctly visualizing the internal layers of roots cells, making it impossible in practice to reveal the presence of FNCs. In addition, the low axial resolution of the system did not allow to ascertain the presence of FNCs inside root hair. As a consequence, LSM was not suited for detailed imaging of the inner cells of the root and the poor axial resolution did not allow to establish the presence of particles inside the root hair.
The control did not show any fluorescent particles.

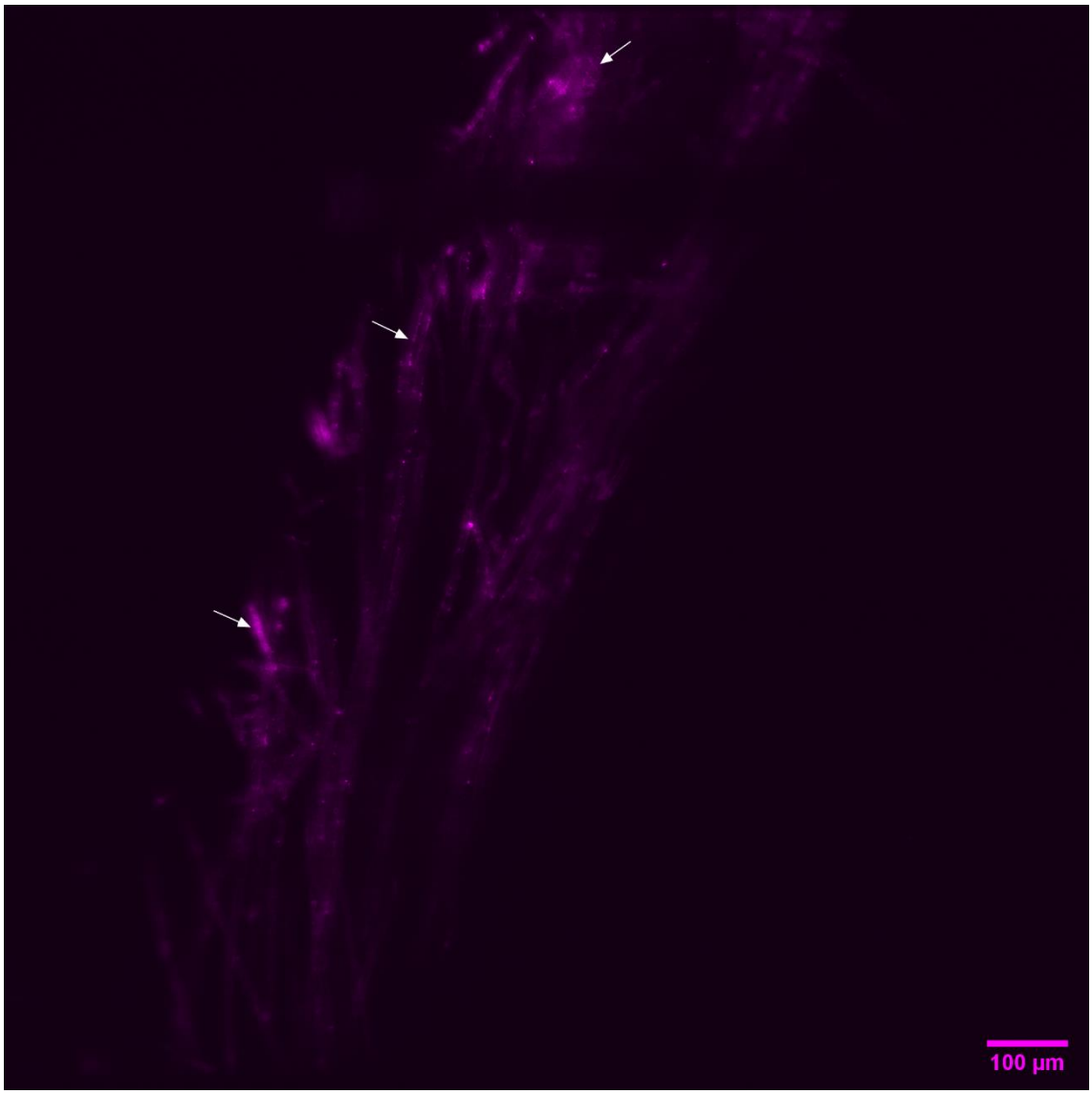

Figure 16. LSM external view of roots hair showing a large quantity of FNCs on their surface. White arrows indicate clusters of FNCs.

Figure 17. LSM focal plane internal to the root, showing clustered FNCs adhering to the outer surface of the root cells. Shadowing effects are also visible at the bottom of the image, while the scattering from the cell walls and outer hair denies the penetration of light into the deeper cells of the root, resulting in blur and poor signal. White arrows indicate external presence of FNCs.

4.2.2 Two-photon microscopy

Two-photon microscopy, thanks to the use of an infrared laser, allows excitation light to penetrate deeper into tissues and offers higher axial and lateral resolution compared to LSM. For these reasons, the technique was tested for *in vivo* imaging of a two weeks old *Eruca sativa* seedling exposed to the 1% lignin pH 11.7 FNCs emulsion diluted 1:5 v/v in dH_2O, with the sample prepared as described in 3.5.1 (Figure 13).

The obtained images resulted in better optical sectioning capability compared to LSM and, as a consequence, it was possible to observe the cell wall structure of the cells at higher depth into the roots. The data showed a large amount of FNCs adhering to the root

epidermis cells and mucilage and to the hair. In addition, it was possible to locate FNCs inside some of the root epidermis cells, while no presence of nanocapsules was observed in the inner cells (Figure 18 and Figure 19). The bigger particles are probably clusters of particles. It is important to notice that despite both cell walls and FNCs emission is in the green spectrum, the signal-to-background of FNCs is high enough to distinguish them with ease in the image.

The control did not show any fluorescent elements neither outside nor inside root cells.

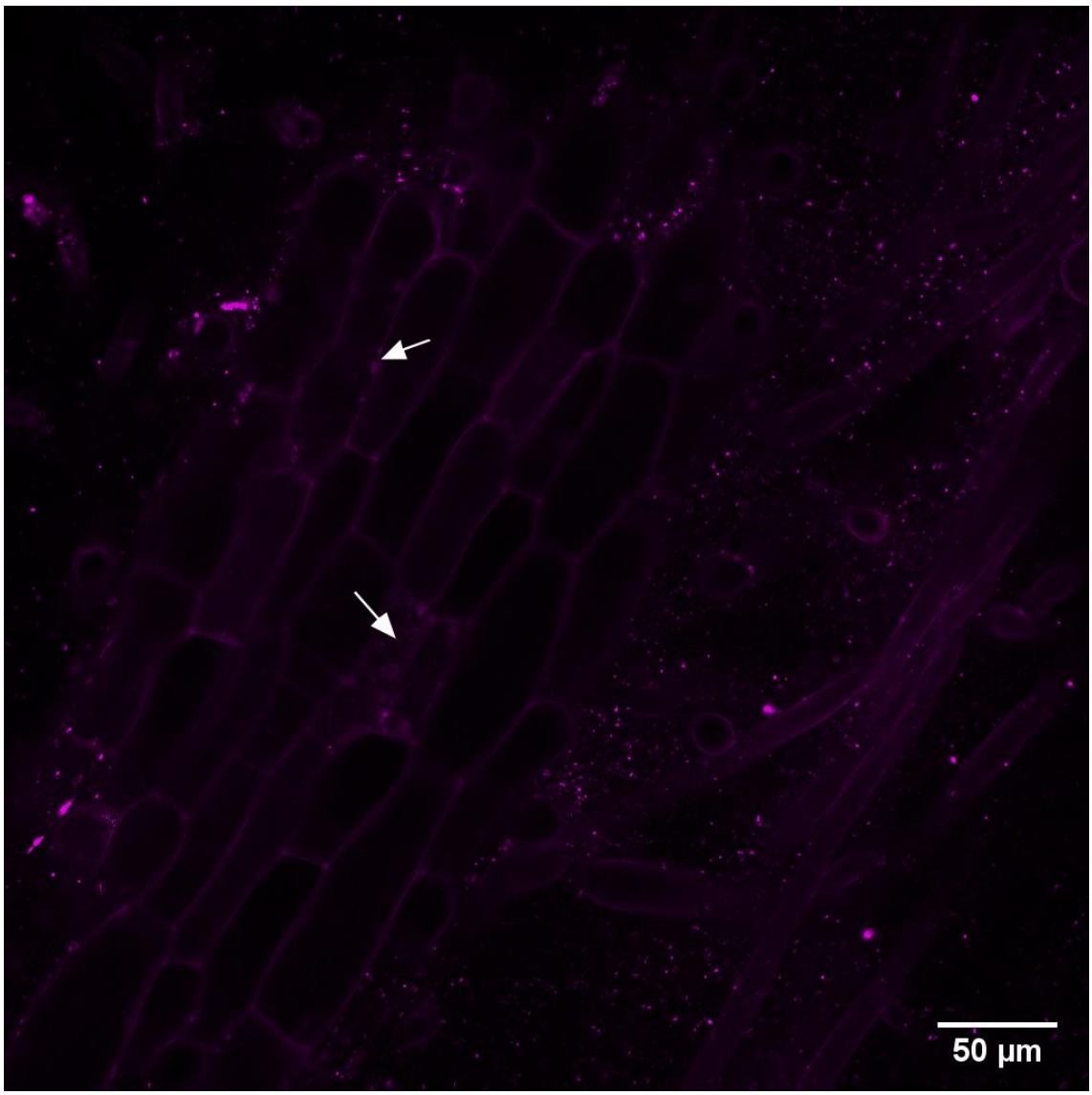

Figure 18. Optical section of the outer layer of cells of *Eruca sativa* root epidermis. A large amount of FNCs can be seen trapped among the external root hair and the surrounding mucilage. White arrows indicate some of the external epidermis cells containing FNCs.

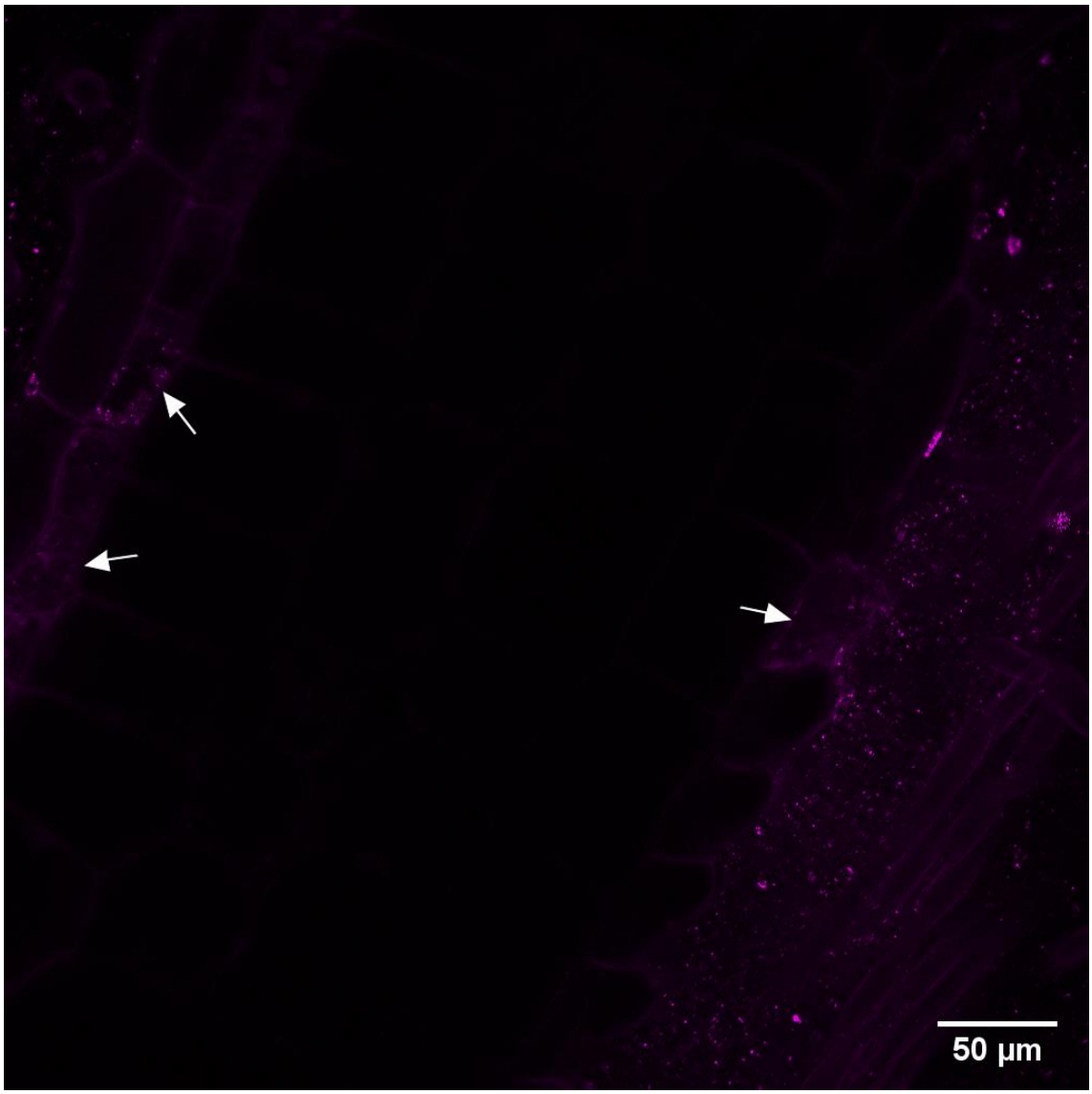

Figure 19. Optical section approximately 66µm deep from *Eruca sativa* root epidermis. White arrows indicate some of the epidermis cells containing FNCs, while no presence of nanocapsules can be observed in the inner cells. Some of the external cells (on the right) show signs of shrinking.

4.3 Additional 2PEFM experiment on *Eruca sativa* and *Eragrostis tef*

As two-photon microscopy revealed to be a suitable tool for the task, a second experiment was set up to better evaluate the entity of the uptake of FNCs which was observed with the preliminary experiment. For this test, two weeks old *Eruca sativa* and *Eragrostis tef* seedlings were put in contact in Eppendorf vials with the 1% lignin pH 11.7 emulsion diluted 1:5 v/v in dH_2O and incubated for 24, 48 and 72 hours. Three plants for each species were exposed for each amount of time, for a total of 18 plants. The controls were taken from the plants incubated as reported in (3.1) and samples were prepared as described in 3.5.1 (Figure 13).

The acquired data revealed that all *Eruca sativa* samples contained FNCs in both epidermis and internal root cells in variable quantity, but not in the vessel elements, as well as adhering in large quantity to the external epidermis and hair. The highest presence was observed in one of the 48h exposition samples and in one of the 72h exposition samples (Figures 20 and 21). Small segments of their roots have been cut and fixed as described in (3.5.2) for TEM imaging. Some of the epidermis cells showed evidence of shrinkage probably due to plasmolysis and cell death or mechanical damage (Figure 22). Quantitative analysis of the presence of FNCs was not possible due to the high signal coming from the particles outside the root and for the presence of many artifact black vertical stripes as an effect of the saturation of the photomultiplier (PMT). This circumstance occurred as it was necessary to set a high gain of the PMT to be able to catch the low signal from the autofluorescence of cell walls to be able to visualize them. As a consequence, the high signal from the abundant FNCs outside the root, still adhering despite the washing steps (probably due to the presence of mucilage), caused the saturation of the PMT and the artifacts.

Eragrostis tef seedlings imaging showed a small presence of FNCs in some epidermis cells in only one of the samples, while many capsules were still adhering outside the epidermis and on their hair.

The controls did only show cell walls autofluorescence and no presence of FNCs.

Due to the large amount of data, only a selection of the most representative frames has been reported in figures.

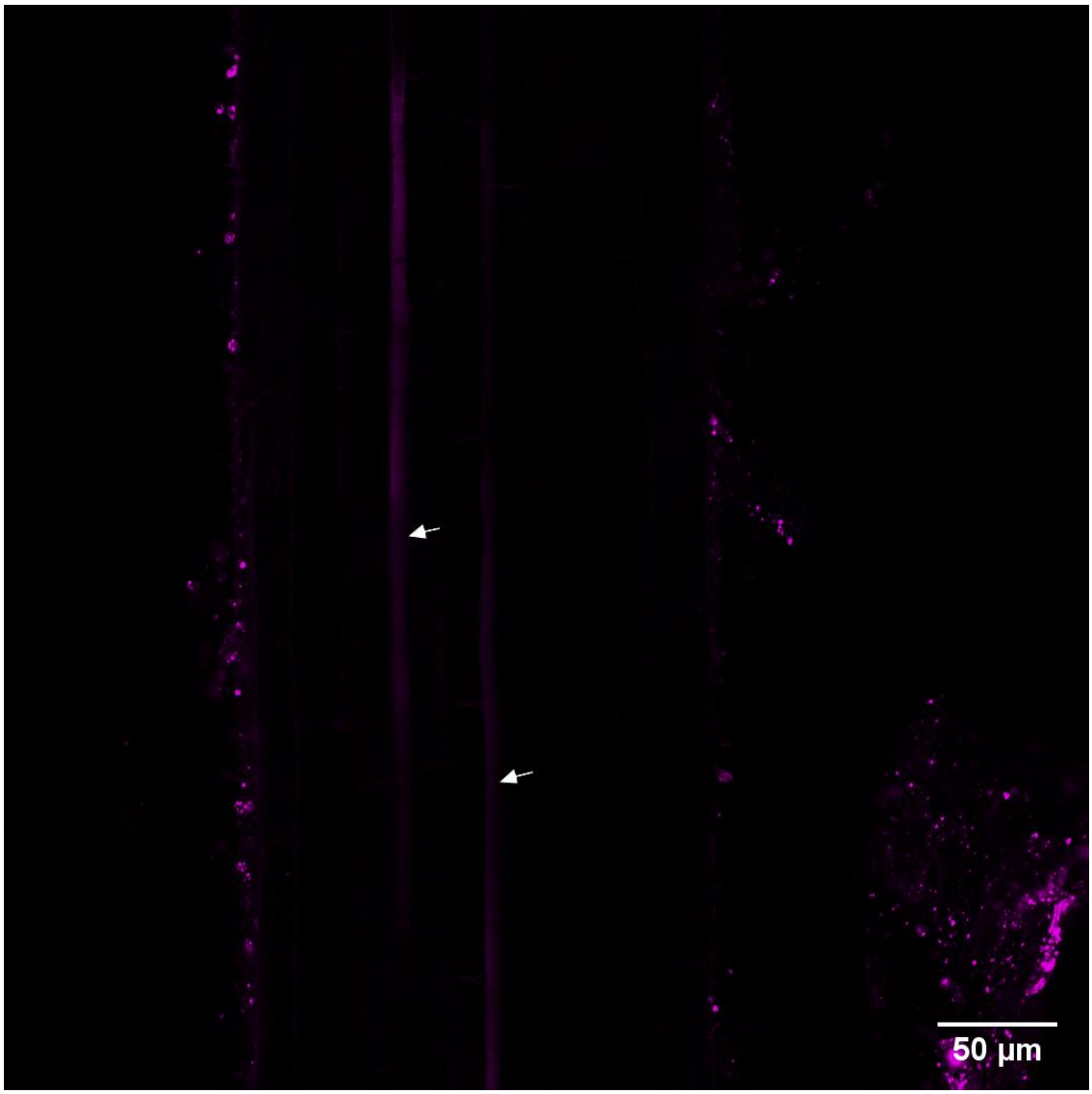

Figure 20. *Eruca sativa* root after 48h exposure to the FNCs emulsion. Optical section about 40µm from the epidermis. A large amount of FNCs can be seen adhering outside the root, while the white arrows show internal cells where FNCs have been internalized.

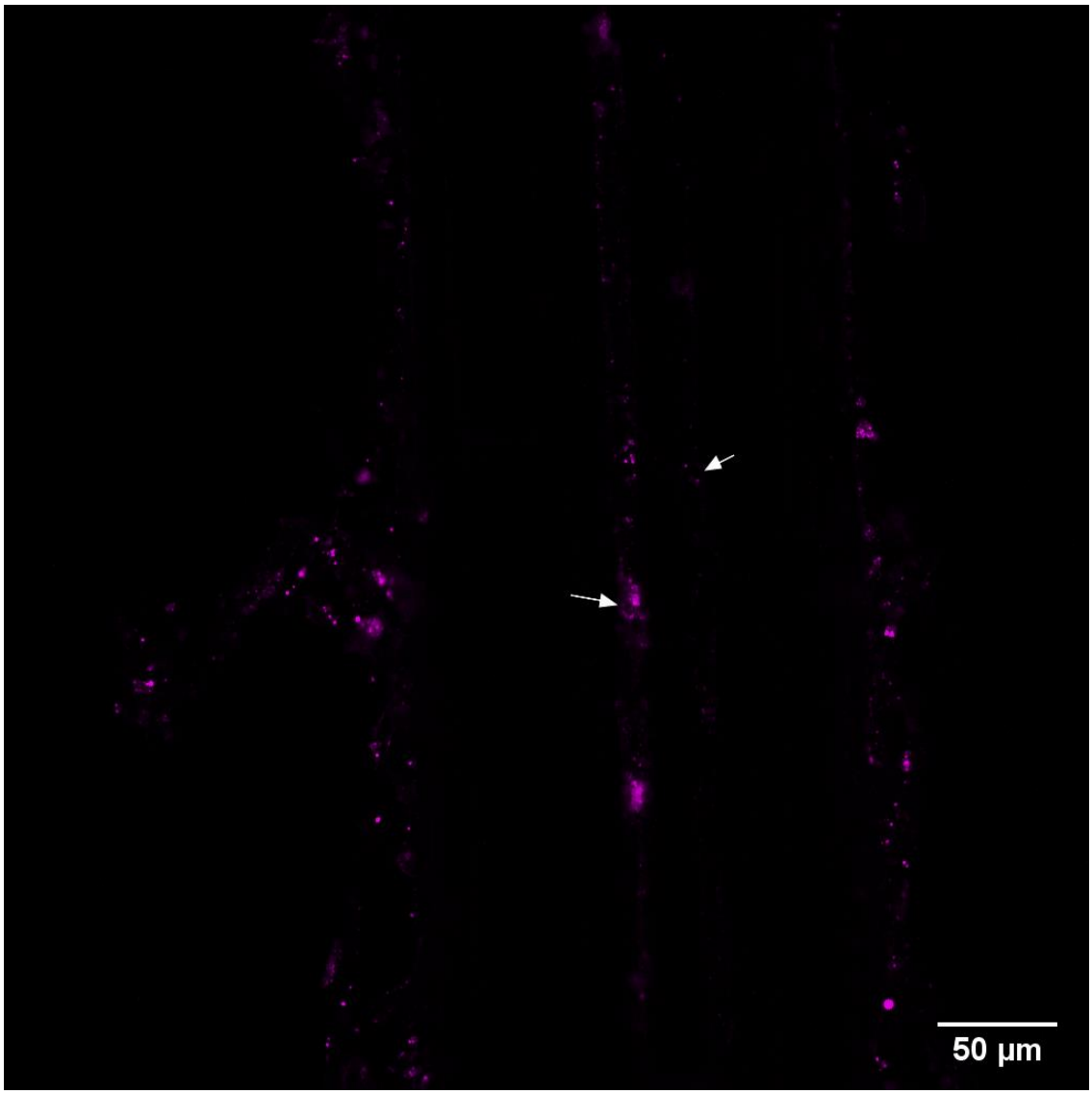

Figure 21. *Eruca sativa* root after 72h exposure to the FNCs emulsion. Optical section about 50µm from the epidermis. As in the previous figure, white arrows indicate internalized FNCs in inner cells.

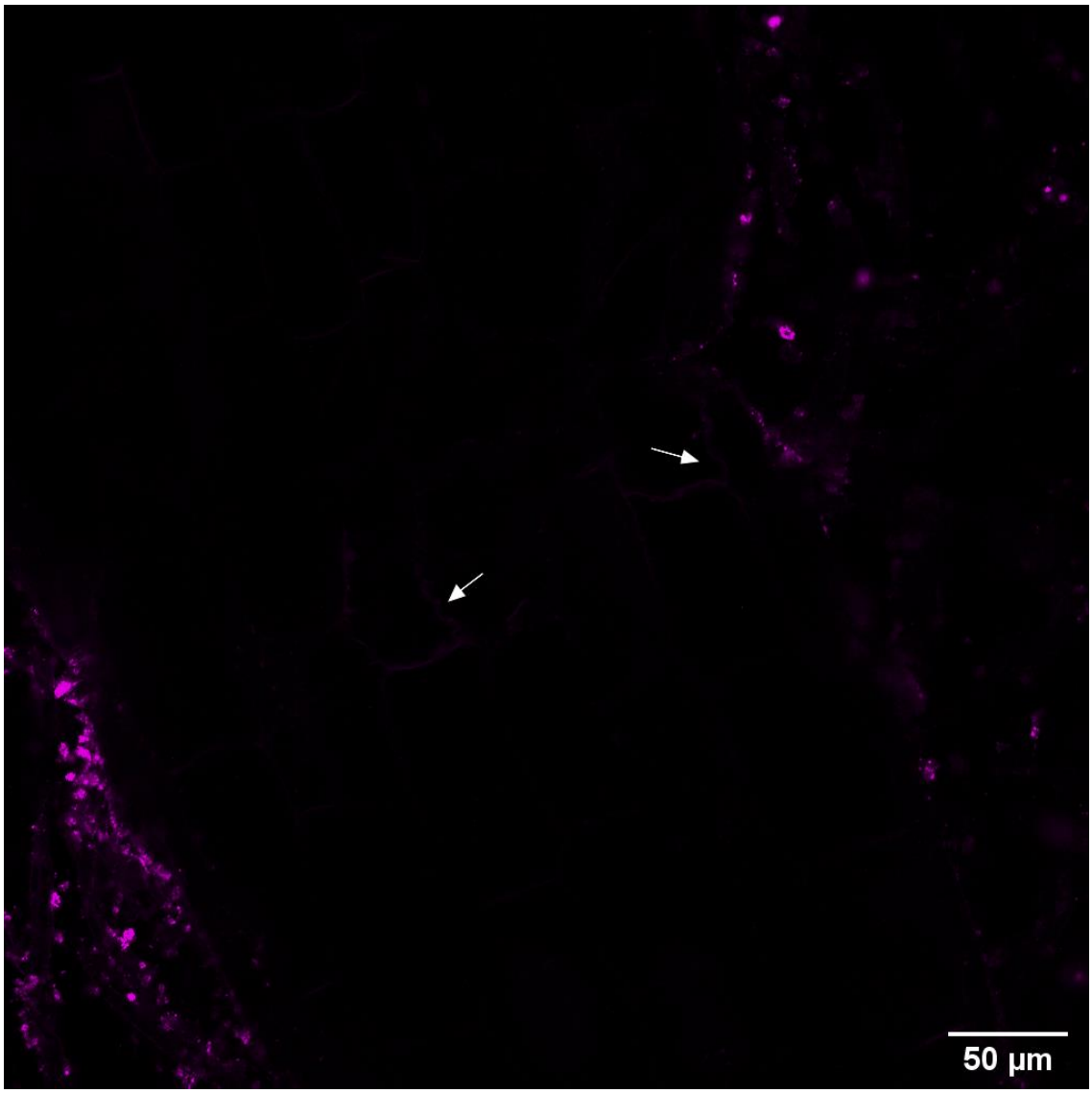

Figure 22. *Eruca sativa* root epidermis cells showing folded cell walls and shrinkage probably due to cell death (white arrows).

The experiment confirmed the internalization of FNCs, especially in *Eruca sativa*, but also revealed the presence of some dead cells which requires further investigations.

4.4 TEM imaging *of Eruca sativa* roots

Segments of the roots dissected from 48h and 72h exposition of *Eruca sativa* seedlings observed with two-photon microscopy as reported in (4.3) were prepared for TEM imaging as described in (3.5.2). In addition, roots from control plants incubated as described in (3.1) were also prepared for the observation. TEM was used to visualize the fine structure of the capsules and the ultrastructure of the cells containing them and eventually identify vesicles membranes which might have included FNCs by endocytosis.

The obtained images allowed us to observe the structure of the FNCs, consisting of a hollow lignin shell showing jagged external surface, reflecting the highly branched structure of lignin (Figure 23).

Many capsules have been found in longitudinal sections of the roots, characterized by variable size and shape, ranging from round to oblong. An almost complete absence of cell ultrastructure was observed in the cells containing the capsules, which must be due to cell death, while cell walls were clearly visible thanks to the potassium permanganate staining (Figure 24). As opposite, the control which was not exposed to the FNCs emulsion, did show typical ultrastructure membranes and structures like nuclei, Golgi apparatus, ribosomes and vesicles could be identified (Figure 25).

The results obtained so far suggest that the 1:5 diluted FNCs emulsion might result toxic for plants and cause cell death, especially in *Eruca sativa*, and led to additional experiments where different dilutions have been tested.

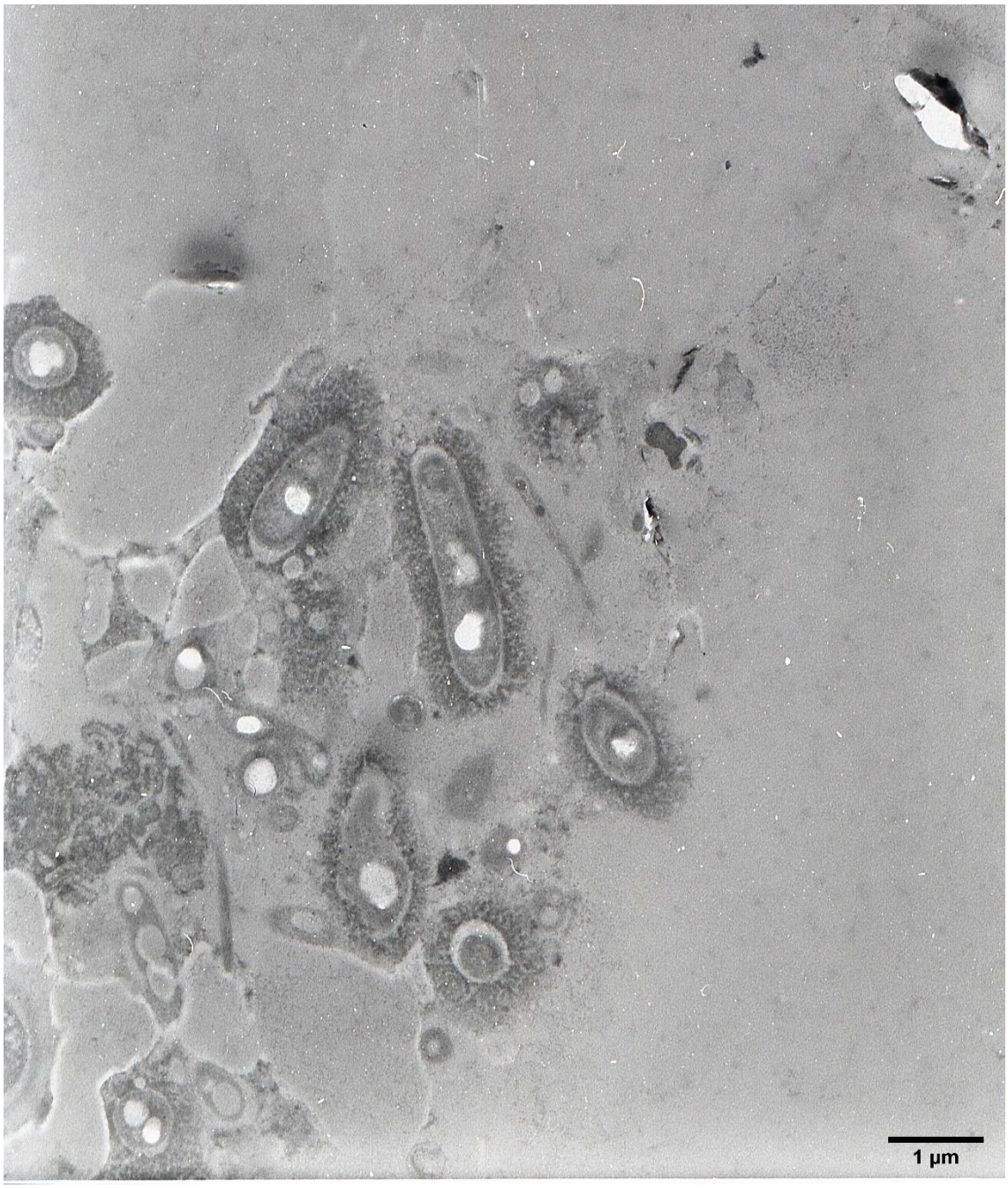

Figure 23. TEM image showing NCs on the external surface of *Eruca sativa* root dissected from the sample used in two-photon imaging. Notice the hollow structure and the jugged margins of the shells. Size and shape are variable.

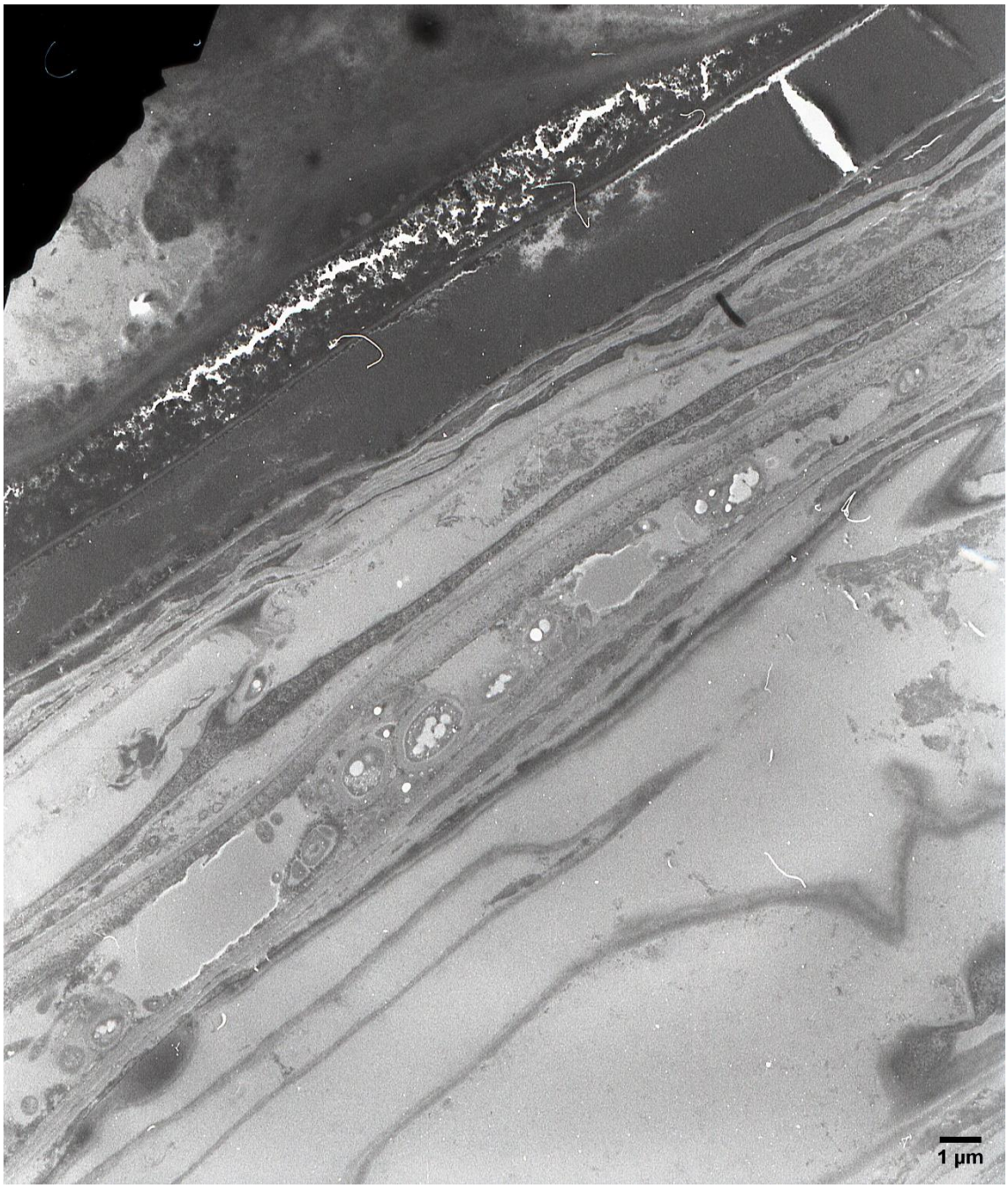

Figure 24. TEM image showing NCs in a longitudinal section of *Eruca sativa* root dissected from the sample used in two-photon imaging. While cell walls are clearly visible, no ultrastructure is evident.

Figure 25. TEM image of a cross section of *Eruca sativa* root belonging to the control. Cell walls and ultrastructure are clearly visible.

4.5 Confocal microscopy experiments

The previous experiments revealed that FNCs can be found in root cells upon administration of the 1:5 diluted FNCs emulsion to *Eruca sativa* seedlings, while *Eragrostis tef* did not seem to internalize them in a considerable amount. Along with this, signs of cell shrinkage and death were observed in two-photon microscopy and TEM images. Further investigations by confocal microscopy were carried on to test the toxicity of the 1:5 diluted FNCs emulsion and different dilutions and to evaluate FNCs uptake. In addition, considering particles size the main hindrance to their internalization, seedlings have been exposed to emulsions filtered by 0.45μm and 0.20μm syringe filters in order to select the smallest fraction of the capsules.

4.5.1 Testing toxicity with propidium iodide

Propidium iodide (PI) is a membrane-impermeable fluorescent dye ($497_{ex}/617_{em}$) which binds to nucleic acids and can be used to spot apoptotic cells. The rupture of plasma membrane in plant apoptotic cells allows the diffusion of the dye inside the cell and its binding to nuclei and other nucleic acids (included mitochondrial DNA). The fluorescence of the dye increases up to 30-fold when bound to nucleic acids.
In this experiment, 9 days old seedlings of *Eruca sativa* and *Eragrostis tef* incubated as reported in (3.1) have been exposed to the same 1:5 dilution of FNCs emulsion used in the two-photon experiment (4.3) for 24, 48 and 72 hours. Plants were put in larger glass containers instead of Eppendorf vials to ease their placement and avoid accidental root mechanical damage by tweezers handling and abrupt bends of the roots which might cause the rupture of cells. Before imaging, seedlings were washed in tap water and incubated for 15 minutes in a propidium iodide solution obtained by adding 5μl/ml from a stock solution containing 1mg/ml of PI (Sigma Aldrich) in tap water. Seedlings were then mounted on microscope slides for *in vivo* imaging as described in (3.5.1). Seedling of each species which were not put into contact with the FNCs emulsion were also incubated for 15 minutes in PI as control. All seedlings have been washed twice in tap water before imaging.
A lambda scan was performed on FNCs from the administered emulsion prior to imaging to finely tune the acquisition spectrum to that of FNCs (the microscope recording system has 5nm spectral resolution) and revealed a peak emission of the nanocapsules at 510nm.

During the imaging, the signal from both the FNCs and PI channels were recorded to visualize apoptotic cells and FNCs at the same time.

Imaging of *Eragrostis tef* roots revealed sparce apoptotic epidermis cells, while no internalization of FNCs was observed in any of the 24, 48 and 72h incubated plants.

Eruca sativa plants showed clear evidence of shrinkage (Figure 27d) and cell death in every sample, with an increment in the severity of the damage after longer exposure times to the emulsion. Apoptotic cells were identified by the detection of PI fluorescence from nuclei (Figure 26, 27) as well as some other apoptotic bodies probably derived by the fragmentation of the nucleus or by the staining of mRNA by PI (Weir, 2001). In addition to root cells, many apoptotic and collapsed hair were observed. The shrinkage of the cells was evident in the brightfield image as well.

The simultaneous observation of the two channels (FNCs+PI signal) allowed to detect the presence of FNCs inside some of the epidermis and inner apoptotic cells (Figure 27c and 28), confirming the hypothesis of toxicity of the emulsion arised from the two-photon experiment (4.3) and TEM observations (4.4). FNCs were observed in abundance adhering to the epidermis and hair as in the previous experiments.

Both *Eruca sativa* and *Eragrostis tef* controls (Figure 29) did not exhibit PI internalization and staining of cytoplasmic nucleic acids, revealing that plants which were not put in contact with the FNCs emulsion have not been damaged.

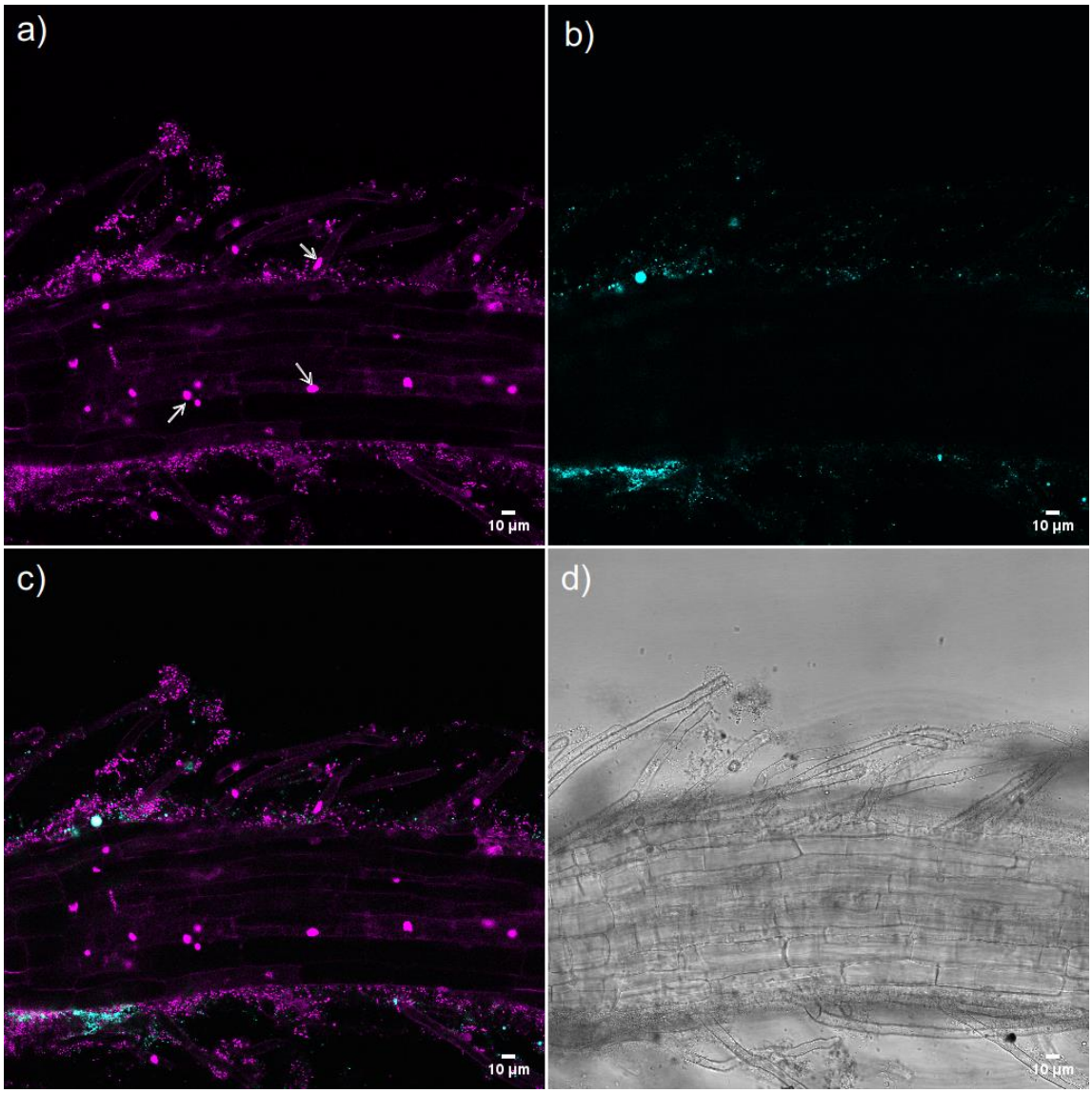

Figure 26. CLSM optical section of *Eruca sativa* root after 48h exposition to the 1:5 FNCs emulsion about 6 µm from root surface; a) PI fluorescence revealed nuclei of apoptotic epidermis cells (white arrows) and hair; b) fluorescence from FNCs adhering to the epidermis and hair; c) overlay of a) and b); c) widefield image.

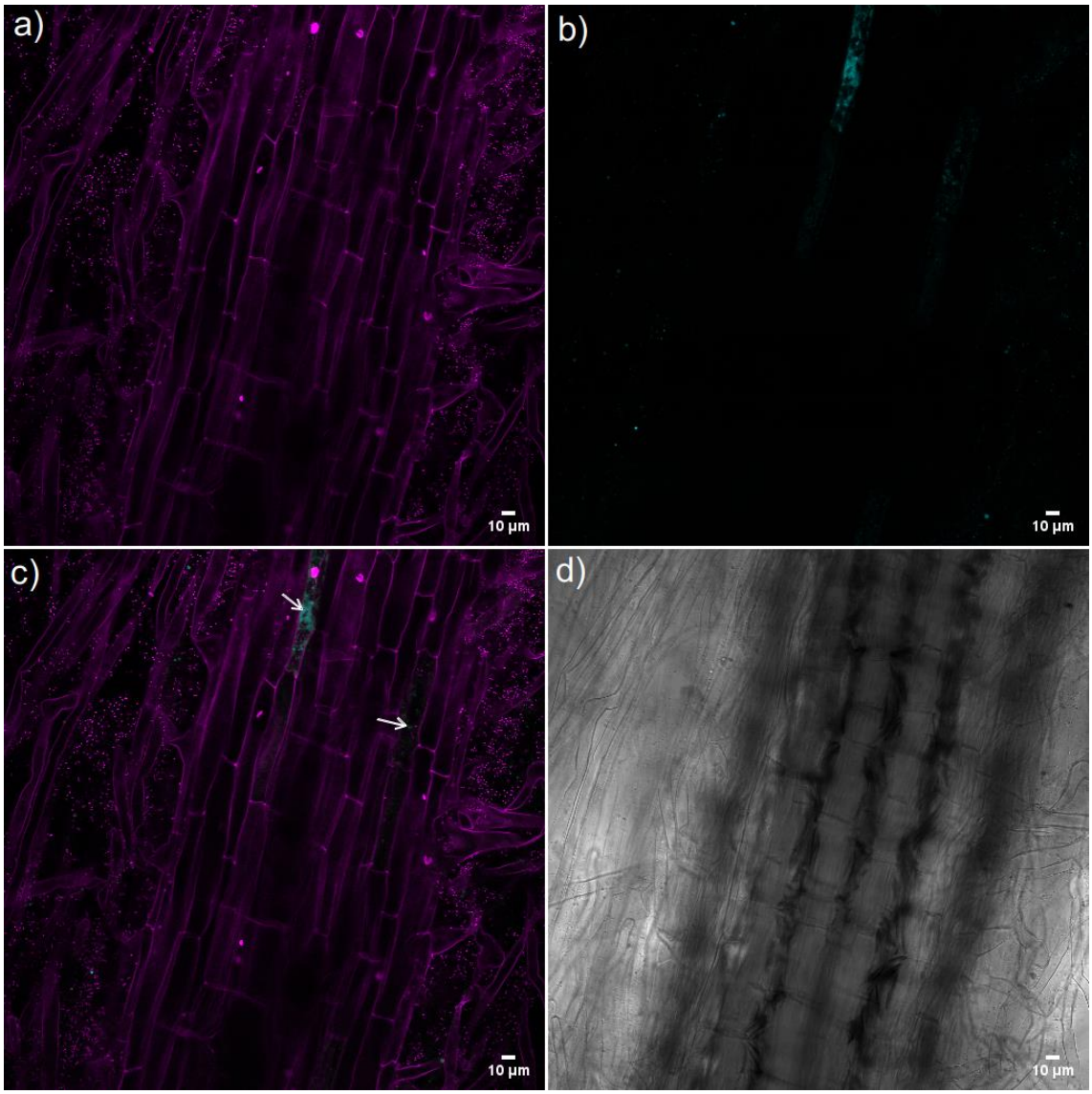

Figure 27. CLSM optical sections of *Eruca sativa* root after 72h exposition to the 1:5 FNCs emulsion; a) PI reveals nuclei of apoptotic cells; b) FNCs were observed inside some apoptotic cells; c) overlay of a) and b) shows the presence of FNCs inside apoptotic cells (white arrows); c) widefield image reveals severe shrinking of cells and collapsed hair.

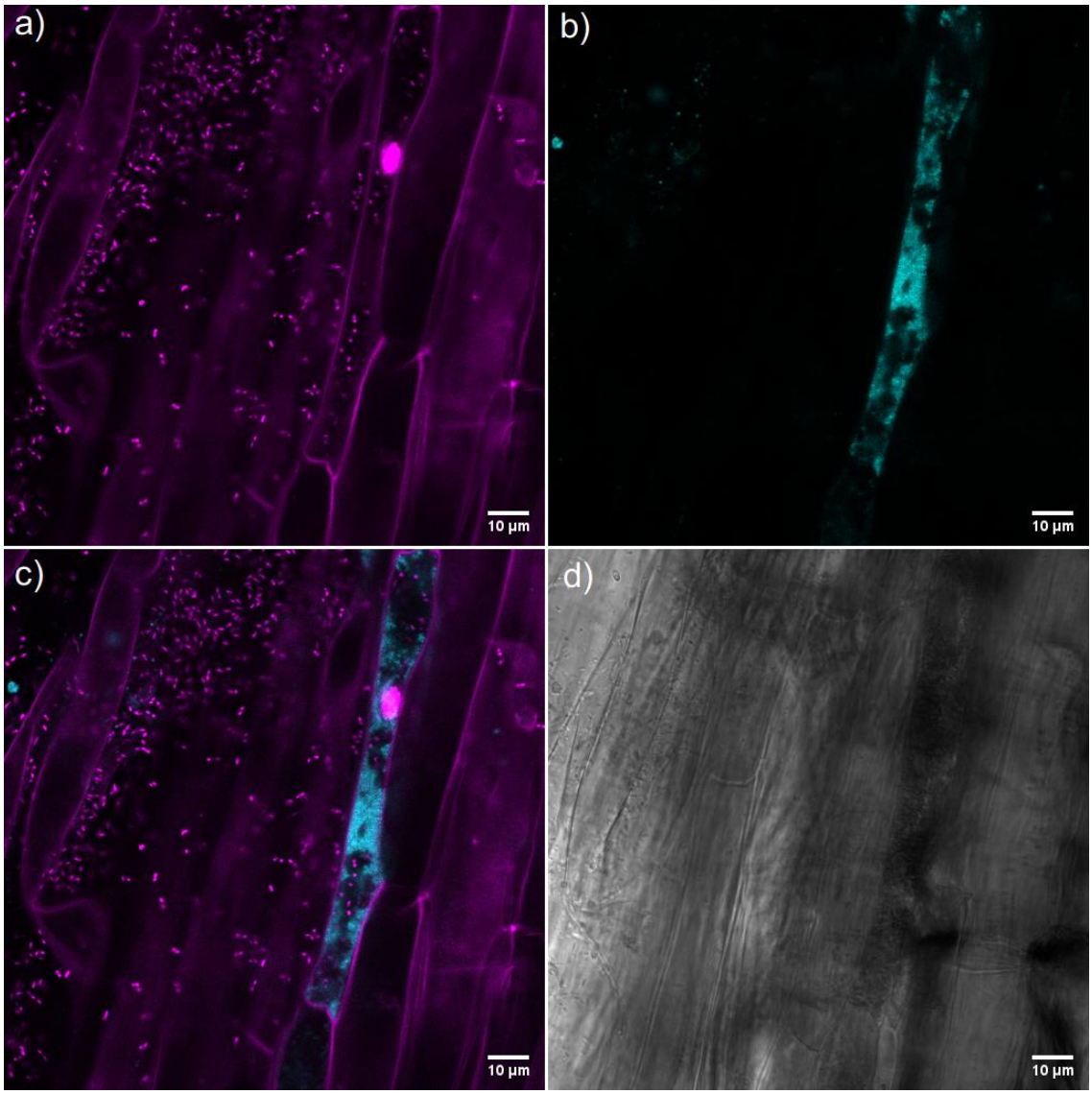

Figure 28. CLSM optical sections of *Eruca sativa* root after 72h exposition to the 1:5 FNCs emulsion; a) apoptotic cell revealed by PI fluorescence from the nucleus; smaller particles are probably PI bound fragments of nuclei or mitochondria totally or partially leaked from apoptotic cells. Chances for fluorescence from eventual contamination by bacteria is low as these particles were not visible in the control (Figure 29); b) FNCs fluorescence from particles inside apoptotic cell; c) overlay of a) and b) revealing the presence of FNCs inside apoptotic cell; c) widefield image.

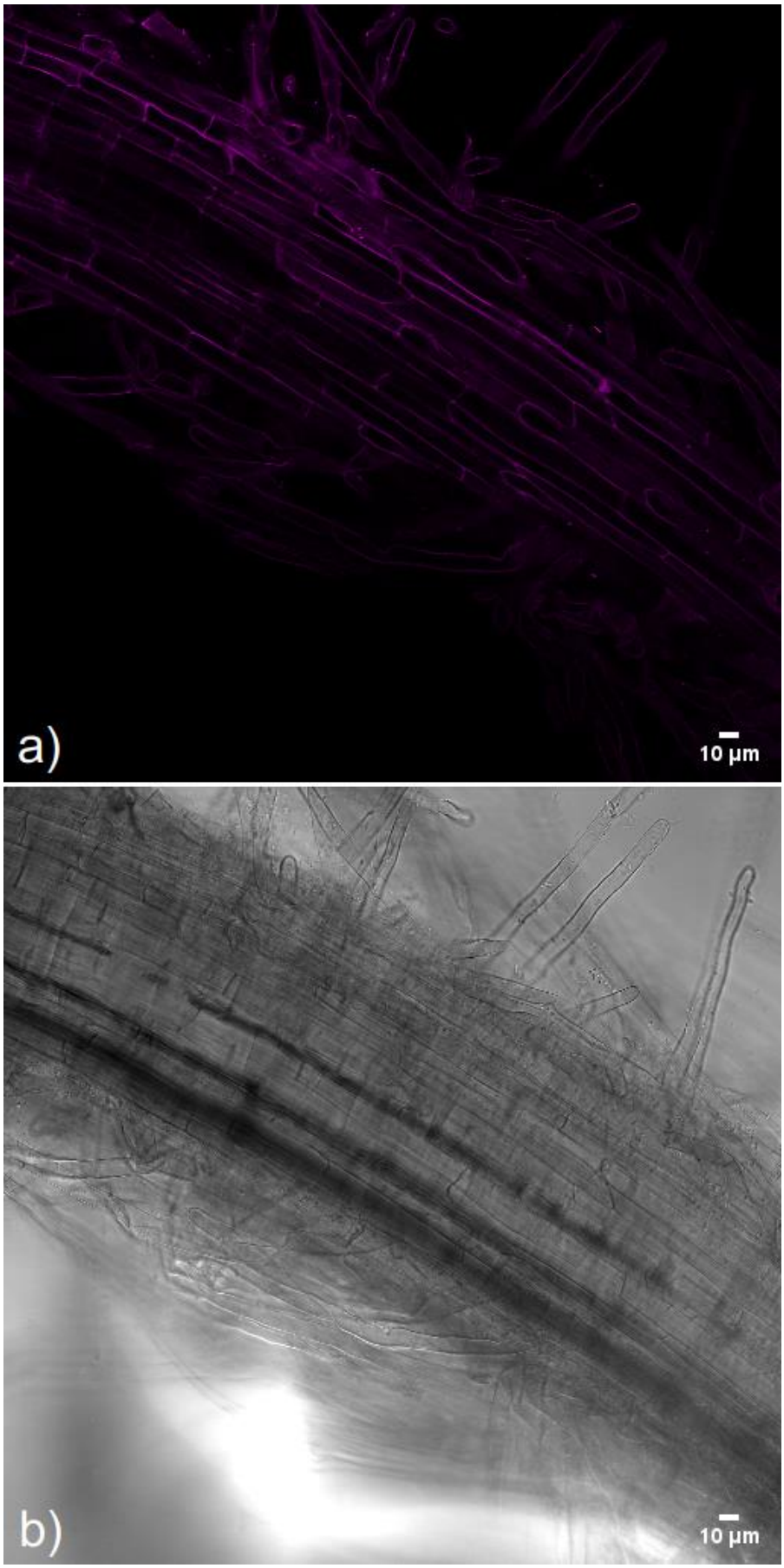

Figure 29. CLSM optical sections of *Eruca sativa* control; a) PI did not stain nuclei or nucleic acids from other organelles, indicating vital cells; b) widefield image shows no evidence of cell shrinkage or collapsed hair.

4.5.2 Toxicity and uptake test at different dilutions

Previous experiments revealed a toxic effect on plants of the 1:5 v/v diluted 1% lignin FNCs emulsion and also demonstrated that nanoparticles toxicity can be species-specific as reported by Faisal et al., 2018. To address this, new experiments were undertaken by administering higher dilutions of the original FNCs emulsion. In addition, the emulsion has been filtered through a 0.45μm and successively a 0.20μm syringe filter to exclude the higher size fraction of nanocapsules (3.2.2), as size, together with chemical composition, is the main factor affecting nanoparticles uptake (Pérez-de-Luque, 2017).
Toxicity and uptake were tested upon administration of a filtered 1:100 v/v dilution in tap water to two weeks old *Eruca sativa* and *Eragrostis tef* seedlings and on one week old *Arabidopsis thaliana* seedlings. DSL analysis of such emulsion is reported in Figure 7 and shows a size peak at 125nm. Imaging was performed after 72h exposition to the emulsion and revealed no signs of apoptosis, but also no evidence of FNCs internalization in cells in any of the species (Figure 30 and 31). FNCs were observed adhering to the external epidermis cell walls and root hair.
The experiment was replicated on two weeks old *Eruca sativa* and *Eragrostis tef* exposed to extruded FNCs emulsion as described in (3.2.3) with analogous results.

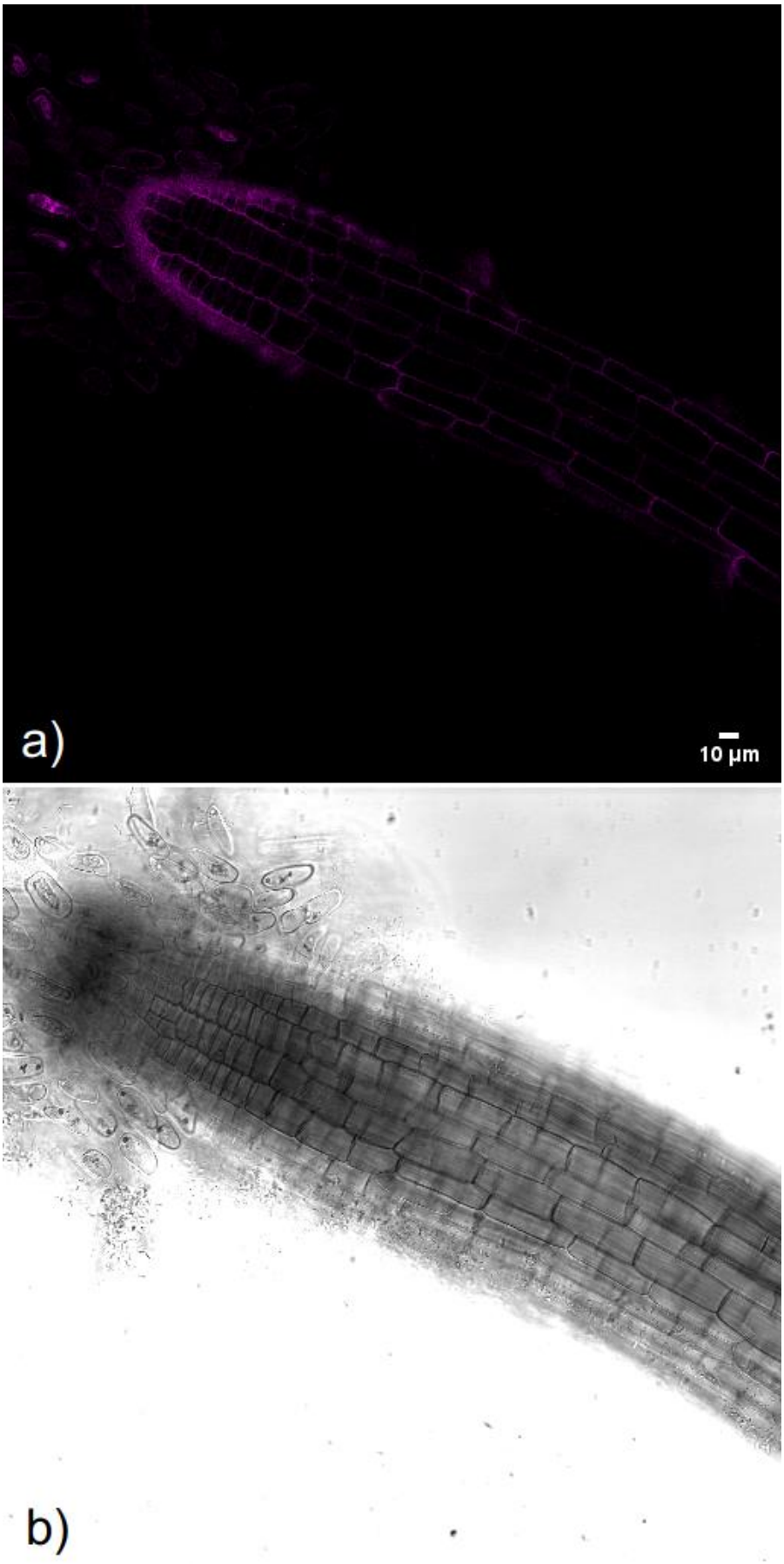

Figure 30. CLSM optical section of *Eruca sativa*; a) no FNCs signal from inner cells was observed; b) widefield image shows no evidence of cell apoptosis, cells are turgid and lively.

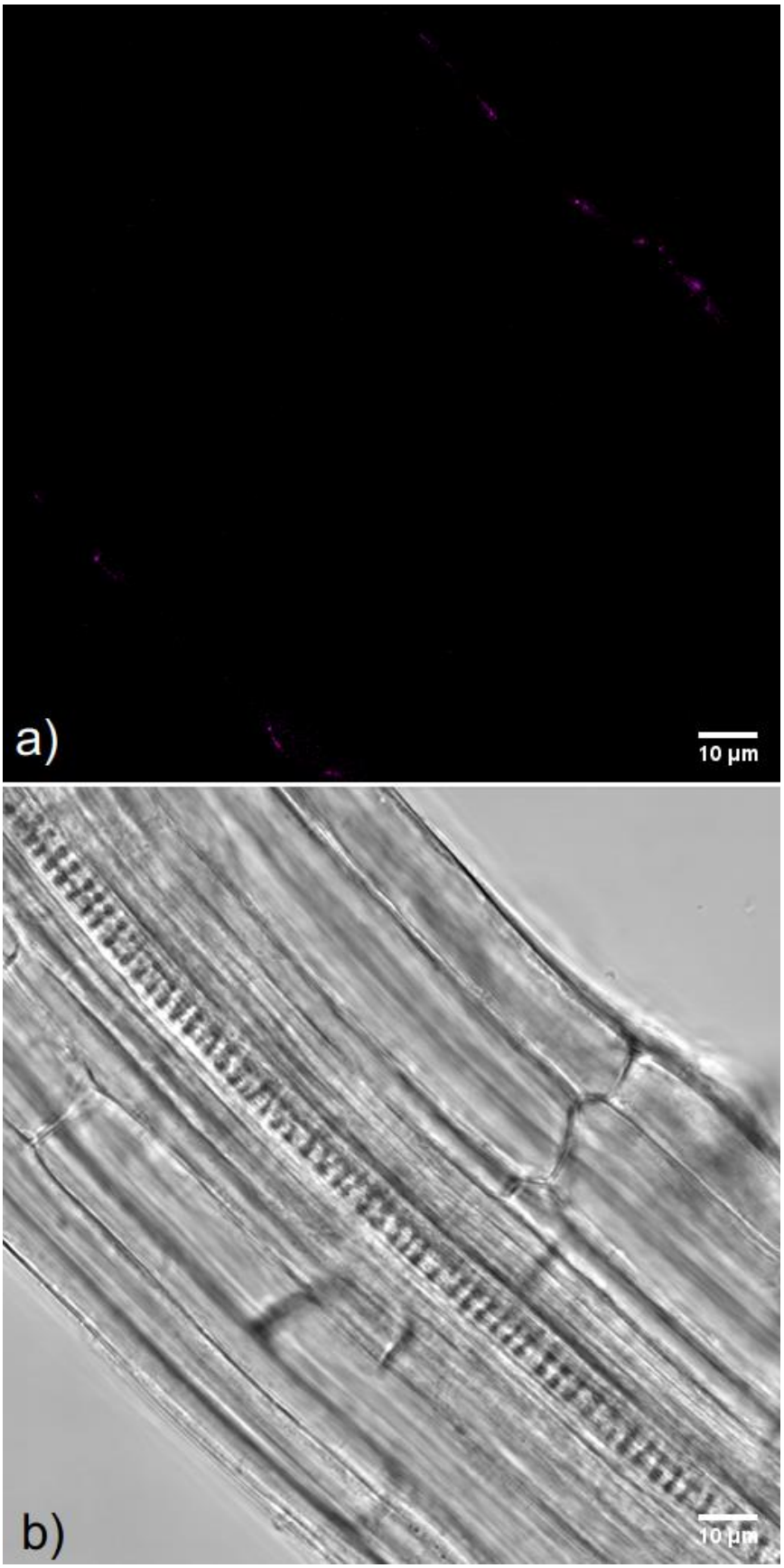

Figure 31. CLSM optical section of *Arabidopsis thaliana*; a) FNCs have been localized only adhering to the outer surface of the root, while no evidence of internalization was observed in cells and xylem vessel does not contain FNCs; b) widefield image shows intact, lively cells.

5. Discussion

The present study tested the viability of lignin NCs produced by ultrasonication (3.2) as nanovectors for the delivery of bio-active compounds to plants.

Preliminary experiments (4.2, 4.3) on plants exposed to the 1:5 v/v dilution in dH_2O of 1% lignin FNCs emulsion revealed the presence of FNCs inside epidermis or inner root cells, but at the same time showed evidence of cell apoptosis. TEM images of the plants exposed to such emulsion confirmed the absence of observable ultrastructure in cells containing the nanocapsules, while cells belonging to the control showed clear ultrastructure details. The experiment with propidium iodide as a cell apoptosis marker (4.5.1) represented the decisive proof that apoptosis in root cells and hair is consistent as a consequence of the exposure to the FNCs 1:5 emulsion. In addition, the overlay of the observed internalized FNCs and the PI channel (Figure 27 and 28) demonstrated that the presence of FNCs only occurs in apoptotic cells of the tested plants and that toxicity in *Eragrostis tef* resulted considerably lower than in *Eruca sativa*, confirming the species-specific effects of nanoparticles which have already been reported in literature (Usman et al., 2020).

As a consequence of the proven adverse effects of the 1:5 FNCs emulsion, a 1:100 v/v in dH_2O dilution has been used to limit the toxicity and verify the uptake of nanocapsules by plants. In addition, as previous experiments did not show any internalization of FNCs in living cells and considering the size of the particles as one of the most critical aspects involved in the success of their uptake, the smaller fraction of the nanocapsules was separated by filtration and extrusion (3.2.2, 3.2.3) prior to the administration in the upcoming experiments. Confocal microscopy imaging of the plants exposed to the highly diluted, 1:100 FNCs emulsion showed no detrimental effects on cells vitality, but at the same time there was no evidence of FNCs uptake (4.5.2).

The study established that the NCs emulsions produced with the described protocol can be toxic for plant cells at high concentrations and their uptake does not occur in living root cells upon administration of any of the tested emulsions.

Addressing the cause of toxicity to a specific factor is not possible with the available data and may require further inquiries. However, some elements can be considered. The eventual presence of leftovers of acetone used during the production process might be a cause, but its high volatility probably determined its total evaporation during the sonication process. A second element of toxicity could be derived by the presence of free fluorescent dye (FY088) in the final emulsion at a high enough concentration to cause

detrimental effects on cells. Lastly, the eventual toxicity of lignin for plants is the less plausible cause, being lignin a fundamental polymer of cell walls naturally synthesized by plants.

As the main factors determining the toxicity of the nanocapsules emulsion used in this study require additional investigations, the missed uptake of the particles is to be attributed with reasonable confidence to their size. The efforts made to select the smallest size fraction of the NCs, did not yield any consistent result uptake-wise. Uptake of particles ranging from less than 10nm up to 30nm has been reported in literature (Corredor et al., 2009; González-Melendi et al., 2008; Sabo-Attwood et al., 2012) and a size of 50nm has been determined by some authors as the exclusion limit (Pérez-de-Luque, 2017). According to this, future design of nanovectors should focus on the development of production processes leading to smaller-sized particles.

In conclusion, we can assert that the application of nanotechnology to agriculture has a high potential towards more sustainable practices which could limit the environmental impact of human food production activities. The engineering of effective nanovectors will open new frontiers for agriculture and the role of research in this field will be decisive in the upcoming years.

6. Acknowledgments

I would like to thank Prof. Alessio Papini for letting me join his lab for my thesis project and my supervisor Sara Falsini for inspiring and supporting my work. I addition, for their joint collaboration to the project, I would also like to thank Prof. Sandra Ristori of the Chemistry Department for providing the sonicator and the DLS analysis, Prof. Cristina Gonnelli of the Plant Physiology Department and Dr. Silvia Schiff for their valuable contribution.

My sincere thanks go to Corrado Fani and Pietro di Falco for their precious technical support during the experiments and to Dr. Irene Costantini from the European Laboratory for Non-Linear Spectroscopy for her assistance during two-photon imaging.

A special thank goes to Giovanni Stefano for his help with confocal imaging and for his precious help in setting up the experiments, for image interpretation and for his hints about plant uptake processes.

I would also want to express my gratitude to BIMA coordinators, Raili Kronström and Joanna Pylvänäinen, for the patience and precious assistance throughout my whole study period in Turku, especially during the recent exceptional circumstances.

My special thanks to Elnaz Fazeli and her kindness for being always present in supporting my studies with her valuable advices.

7. References

A. Werner, J. Stafford (Eds.), 2003. Precision Agriculture. Wageningen Academic Publishers. https://doi.org/10.3920/978-90-8686-514-7

Advanced Applications: Multiphoton [WWW Document], n.d. . Teledyne Photom. URL https://www.photometrics.com/learn/physics-and-biophysics/two-photon (accessed 6.28.21).

Agustin, M.B., Penttilä, P.A., Lahtinen, M., Mikkonen, K.S., 2019. Rapid and Direct Preparation of Lignin Nanoparticles from Alkaline Pulping Liquor by Mild Ultrasonication. ACS Sustain. Chem. Eng. 7, 19925–19934. https://doi.org/10.1021/acssuschemeng.9b05445

Ahmed, A., 2016. Applications of Nickel Nanoparticles for Control of Fusarium Wilt on Lettuce and Tomato. Int. J. Innov. Res. Sci. Eng. Technol. 5, 7378–7385. https://doi.org/10.15680/IJIRSET.2016.0505132

Avellan, A., Schwab, F., Mason, A., Chaurand, P., Borschneck, D., Vidal, V., Rose, J., Santaella, C., Levard, C., 2017. Nanoparticle Uptake in Plants: Gold Nanomaterial Localized in Roots of *Arabidopsis thaliana* by X-ray Computed Nanotomography and Hyperspectral Imaging. Environ. Sci. Technol. 51, 8682–8691. https://doi.org/10.1021/acs.est.7b01133

Aziz, H.M.M.A., Hasaneen, M.N.A., Omer, A.M., 2016. Nano chitosan-NPK fertilizer enhances the growth and productivity of wheat plants grown in sandy soil. Span. J. Agric. Res. 14, 17.

Bahadar, H., Maqbool, F., Niaz, K., Abdollahi, M., 2016. Toxicity of Nanoparticles and an Overview of Current Experimental Models. Iran. Biomed. J. 20, 1–11. https://doi.org/10.7508/ibj.2016.01.001

Banerji, A., Wickner, P.G., Saff, R., Stone, C.A., Robinson, L.B., Long, A.A., Wolfson, A.R., Williams, P., Khan, D.A., Phillips, E., Blumenthal, K.G., 2021. mRNA Vaccines to Prevent COVID-19 Disease and Reported Allergic Reactions: Current Evidence and Suggested Approach. J. Allergy Clin. Immunol. Pract. 9, 1423–1437. https://doi.org/10.1016/j.jaip.2020.12.047

Berthet, B., Maizel, A., 2016. Light sheet microscopy and live imaging of plants. J. Microsc. 263, 158–164. https://doi.org/10.1111/jmi.12393

Briolay, T., Petithomme, T., Fouet, M., Nguyen-Pham, N., Blanquart, C., Boisgerault, N., 2021. Delivery of cancer therapies by synthetic and bio-inspired nanovectors. Mol. Cancer 20, 55. https://doi.org/10.1186/s12943-021-01346-2

Confocal Microscopy - Resolution and Contrast in Confocal Microscopy | Olympus LS [WWW Document], n.d. URL https://www.olympus-lifescience.com/en/microscope-resource/primer/techniques/confocal/resolutionintro/ (accessed 6.28.21).

Corredor, E., Testillano, P.S., Coronado, M.-J., González-Melendi, P., Fernández-Pacheco, R., Marquina, C., Ibarra, M.R., de la Fuente, J.M., Rubiales, D., Pérez-de-Luque, A., Risueño, M.-C., 2009. Nanoparticle penetration and transport in living pumpkin plants: in situsubcellular identification. BMC Plant Biol. 9, 45. https://doi.org/10.1186/1471-2229-9-45

Cunningham, F.J., Goh, N.S., Demirer, G.S., Matos, J.L., Landry, M.P., 2018. Nanoparticle-Mediated Delivery towards Advancing Plant Genetic Engineering. Trends Biotechnol. 36, 882–897. https://doi.org/10.1016/j.tibtech.2018.03.009

Dai, L., Liu, R., Hu, L.-Q., Zou, Z.-F., Si, C.-L., 2017. Lignin Nanoparticle as a Novel Green Carrier for the Efficient Delivery of Resveratrol [WWW Document]. https://doi.org/10.1021/acssuschemeng.7b01903

Dastpak, A., Lourençon, T.V., Balakshin, M., Farhan Hashmi, S., Lundström, M., Wilson, B.P., 2020. Solubility study of lignin in industrial organic solvents and investigation of electrochemical properties of spray-coated solutions. Ind. Crops Prod. 148, 112310. https://doi.org/10.1016/j.indcrop.2020.112310

Demirer, G.S., Chang, R., Zhang, H., Chio, L., Landry, M.P., 2018. Nanoparticle-Guided Biomolecule Delivery for Transgene Expression and Gene Silencing in Mature Plants. Biophys. J. 114, 217a. https://doi.org/10.1016/j.bpj.2017.11.1209

Deng, Y., Zhao, H., Qian, Y., Lü, L., Wang, B., Qiu, X., 2016. Hollow lignin azo colloids encapsulated avermectin with high anti-photolysis and controlled release performance. Ind. Crops Prod. 87, 191–197. https://doi.org/10.1016/j.indcrop.2016.03.056

Duhan, J.S., Kumar, R., Kumar, N., Kaur, P., Nehra, K., Duhan, S., 2017. Nanotechnology: The new perspective in precision agriculture. Biotechnol. Rep. 15, 11–23. https://doi.org/10.1016/j.btre.2017.03.002

Faisal, M., Saquib, Q., Alatar, A.A., Al-Khedhairy, A.A. (Eds.), 2018. Phytotoxicity of Nanoparticles. Springer International Publishing, Cham. https://doi.org/10.1007/978-3-319-76708-6

Falsini, S., Clemente, I., Papini, A., Tani, C., Schiff, S., Salvatici, M.C., Petruccelli, R., Benelli, C., Giordano, C., Gonnelli, C., Ristori, S., 2019. When Sustainable Nanochemistry Meets Agriculture: Lignin Nanocapsules for Bioactive Compound Delivery to Plantlets. ACS Sustain. Chem. Eng. 7, 19935–19942. https://doi.org/10.1021/acssuschemeng.9b05462

Falsini, S., Tani, C., Schiff, S., Gonnelli, C., Clemente, I., Ristori, S., Papini, A., 2020. A new method for the direct tracking of in vivo lignin nanocapsules in Eragrostis tef (Poaceae) tissues. Eur. J. Histochem. EJH 64. https://doi.org/10.4081/ejh.2020.3112

Faveeuw, C., Trottein, F., 2014. Optimization of natural killer T cell-mediated immunotherapy in cancer using cell-based and nanovector vaccines. Cancer Res. 74, 1632–1638. https://doi.org/10.1158/0008-5472.CAN-13-3504

Frenk, S., Ben-Moshe, T., Dror, I., Berkowitz, B., Minz, D., 2013. Effect of Metal Oxide Nanoparticles on Microbial Community Structure and Function in Two Different Soil Types. PLOS ONE 8, e84441. https://doi.org/10.1371/journal.pone.0084441

Gajjar, P., Pettee, B., Britt, D.W., Huang, W., Johnson, W.P., Anderson, A.J., 2009. Antimicrobial activities of commercial nanoparticles against an environmental soil microbe, Pseudomonas putida KT2440. J. Biol. Eng. 3, 1–13.

Ghidan, Alaa Y, Al-Antary, T.M., Awwad, A.M., Akash, M.W., 2017. APHIDICIDAL POTENTIAL OF GREEN SYNTHESIZED MAGNESIUM HYDROXIDE NANOPARTICLES USING 12, 9.

Ghidan, A.Y., Al-Antary, T.M., Awwad, A.M., Ghidan, O.Y., Araj, S.-E.A., Ateyyat, M.A., 2018. Comparison of different green synthesized nanomaterials on green peach aphid as aphicidal potential. Fresenius Env. Bull 27, 7009–7016.

Ghidan, Alaa Y., Al-Antary, T.M., Salem, N.M., Awwad, A.M., 2017. Facile green synthetic route to the zinc oxide (ZnONPs) nanoparticles: Effect on green peach aphid and antibacterial activity. J. Agric. Sci. 9, 131.

Giguère, P.A., Harvey, K.B., 1956. ON THE INFRARED ABSORPTION OF WATER AND HEAVY WATER IN CONDENSED STATES. Can. J. Chem. 34, 798–808. https://doi.org/10.1139/v56-103

Gilca, I.A., Popa, V.I., Crestini, C., 2015. Obtaining lignin nanoparticles by sonication. Ultrason. Sonochem. 23, 369–375. https://doi.org/10.1016/j.ultsonch.2014.08.021

González-Melendi, P., Fernández-Pacheco, R., Coronado, M.J., Corredor, E., Testillano, P.S., Risueño, M.C., Marquina, C., Ibarra, M.R., Rubiales, D., Pérez-de-Luque, A., 2008. Nanoparticles as Smart Treatment-delivery Systems in Plants: Assessment of Different Techniques of Microscopy for their Visualization in Plant Tissues. Ann. Bot. 101, 187–195. https://doi.org/10.1093/aob/mcm283

Grillo, R., Clemente, Z., Oliveira, J.L. de, Campos, E.V.R., Chalupe, V.C., Jonsson, C.M., Lima, R. de, Sanches, G., Nishisaka, C.S., Rosa, A.H., Oehlke, K., Greiner, R., Fraceto, L.F., 2015. Chitosan nanoparticles loaded the herbicide paraquat: The influence of the aquatic humic substances on the colloidal stability and toxicity. J. Hazard. Mater. 286, 562–572. https://doi.org/10.1016/j.jhazmat.2014.12.021

Gupta, A.K., Mohanty, S., Nayak, S.K., 2014. Synthesis, Characterization and Application of Lignin Nanoparticles (LNPs). Mater. Focus 3, 444–454. https://doi.org/10.1166/mat.2014.1217

Gurr, J.-R., Wang, A.S.S., Chen, C.-H., Jan, K.-Y., 2005. Ultrafine titanium dioxide particles in the absence of photoactivation can induce oxidative damage to human bronchial epithelial cells. Toxicology 213, 66–73. https://doi.org/10.1016/j.tox.2005.05.007

Huang, S., Wang, L., Liu, L., Hou, Y., Li, L., 2015. Nanotechnology in agriculture, livestock, and aquaculture in China. A review. Agron. Sustain. Dev. 35, 369–400. https://doi.org/10.1007/s13593-014-0274-x

Introduction to Electron Microscopy - Advanced Microscopy - Imaging Facilities - The University of Utah [WWW Document], n.d. URL https://advanced-microscopy.utah.edu/education/electron-micro/ (accessed 6.29.21).

Jeevanandam, J., Barhoum, A., Chan, Y.S., Dufresne, A., Danquah, M.K., 2018. Review on nanoparticles and nanostructured materials: history, sources, toxicity and regulations. Beilstein J. Nanotechnol. 9, 1050–1074. https://doi.org/10.3762/bjnano.9.98

Jhanzab, H., Razzaq, A., Rehman, A., Hafeez, A., Yasmeen, F., 2015. Silver nano-particles enhance the growth, yield and nutrient use efficiency of wheat. Int. J. Agron. Agric. Res. IJAAR 7, 15–22.

Khan, Ibrahim, Saeed, K., Khan, Idrees, 2019. Nanoparticles: Properties, applications and toxicities. Arab. J. Chem. 12, 908–931. https://doi.org/10.1016/j.arabjc.2017.05.011

Le Goas, M., Paquirissamy, A., Gargouri, D., Fadda, G., Testard, F., Aymes-Chodur, C., Jubeli, E., Pourcher, T., Cambien, B., Palacin, S., Renault, J.-P., Carrot, G., 2019. Irradiation Effects on Polymer-Grafted Gold Nanoparticles for Cancer Therapy. ACS Appl. Bio Mater. 2, 144–154. https://doi.org/10.1021/acsabm.8b00484

Li, Y., Qiu, X., Qian, Y., Xiong, W., Yang, D., 2017. pH-responsive lignin-based complex micelles: Preparation, characterization and application in oral drug delivery. Chem. Eng. J. 327, 1176–1183. https://doi.org/10.1016/j.cej.2017.07.022

Lievonen, M., Valle-Delgado, J.J., Mattinen, M.-L., Hult, E.-L., Lintinen, K., Kostiainen, M.A., Paananen, A., Szilvay, G.R., Setälä, H., Österberg, M., 2016. A simple process for lignin nanoparticle preparation. Green Chem. 18, 1416–1422. https://doi.org/10.1039/C5GC01436K

Liu, R., Lal, R., 2015. Potentials of engineered nanoparticles as fertilizers for increasing agronomic productions. Sci. Total Environ. 514, 131–139. https://doi.org/10.1016/j.scitotenv.2015.01.104

Lu, Q., Zhu, M., Zu, Y., Liu, W., Yang, L., Zhang, Y., Zhao, X., Zhang, Xiunan, Zhang, Xiaonan, Li, W., 2012. Comparative antioxidant activity of nanoscale lignin prepared by a supercritical antisolvent (SAS) process with non-nanoscale lignin. Food Chem. 135, 63–67. https://doi.org/10.1016/j.foodchem.2012.04.070

Madan, H.R., Sharma, S.C., Suresh, D., Vidya, Y.S., Nagabhushana, H., Rajanaik, H., Anantharaju, K.S., Prashantha, S.C., Maiya, P.S., 2016. Facile green fabrication of nanostructure ZnO plates, bullets, flower, prismatic tip, closed pine cone: their antibacterial, antioxidant, photoluminescent and photocatalytic properties. Spectrochim. Acta. A. Mol. Biomol. Spectrosc. 152, 404–416.

MICROSCOPY TECHNIQUES | Electron Microscopy - ScienceDirect [WWW Document], n.d. URL https://www.sciencedirect.com/science/article/pii/B0123693977003848 (accessed 6.29.21).

Mostany, R., Miquelajauregui, A., Shtrahman, M., Portera-Cailliau, C., 2015. Two-photon excitation microscopy and its applications in neuroscience. Methods Mol. Biol. Clifton NJ 1251, 25–42. https://doi.org/10.1007/978-1-4939-2080-8_2

Pérez-de-Luque, A., 2017. Interaction of Nanomaterials with Plants: What Do We Need for Real Applications in Agriculture? Front. Environ. Sci. 5. https://doi.org/10.3389/fenvs.2017.00012

Qian, Y., Deng, Y., Qiu, X., Li, H., Yang, D., 2014. Formation of uniform colloidal spheres from lignin, a renewable resource recovered from pulping spent liquor. Green Chem. 16, 2156–2163. https://doi.org/10.1039/C3GC42131G

Qian, Y., Zhong, X., Li, Y., Qiu, X., 2017. Fabrication of uniform lignin colloidal spheres for developing natural broad-spectrum sunscreens with high sun protection factor. Ind. Crops Prod. 101, 54–60. https://doi.org/10.1016/j.indcrop.2017.03.001

Quesenberry, P.J., Aliotta, J., Camussi, G., Abdel-Mageed, A.B., Wen, S., Goldberg, L., Zhang, H.-G., Tetta, C., Franklin, J., Coffey, R.J., Danielson, K., Subramanya, V., Ghiran, I., Das, S., Chen, C.C., Pusic, K.M., Pusic, A.D., Chatterjee, D., Kraig, R.P., Balaj, L., Dooner, M., 2015. Potential functional applications of extracellular vesicles: a report by the NIH Common Fund Extracellular RNA

Communication Consortium. J. Extracell. Vesicles 4, 27575. https://doi.org/10.3402/jev.v4.27575

Reza, M., Kontturi, E., Jääskeläinen, A.-S., Vuorinen, T., Ruokolainen, J., 2015. Transmission electron microscopy for wood and fiber analysis – A Review. BioResources 10, 6230–6261. https://doi.org/10.15376/biores.10.3.Reza

Royal Society (Great Britain), Royal Academy of Engineering (Great Britain), 2004. Nanoscience and nanotechnologies: opportunities and uncertainties. Royal Society : Royal Academy of Engineering, London.

Sabo-Attwood, T., Unrine, J.M., Stone, J.W., Murphy, C.J., Ghoshroy, S., Blom, D., Bertsch, P.M., Newman, L.A., 2012. Uptake, distribution and toxicity of gold nanoparticles in tobacco (Nicotiana xanthi) seedlings. Nanotoxicology 6, 353–360. https://doi.org/10.3109/17435390.2011.579631

Salata, O., 2004. Applications of nanoparticles in biology and medicine. J. Nanobiotechnology 2, 3. https://doi.org/10.1186/1477-3155-2-3

Sampathkumar, K., Tan, K.X., Loo, S.C.J., 2020. Developing Nano-Delivery Systems for Agriculture and Food Applications with Nature-Derived Polymers. iScience 23, 101055. https://doi.org/10.1016/j.isci.2020.101055

Shankramma, K., Yallappa, S., Shivanna, M.B., Manjanna, J., 2016. Fe2O3 magnetic nanoparticles to enhance S. lycopersicum (tomato) plant growth and their biomineralization. Appl. Nanosci. 6, 983–990. https://doi.org/10.1007/s13204-015-0510-y

Shen, Z., Chen, Z., Hou, Z., Li, T., Lu, X., 2015. Ecotoxicological effect of zinc oxide nanoparticles on soil microorganisms. Front. Environ. Sci. Eng. 9, 912–918. https://doi.org/10.1007/s11783-015-0789-7

Shi, J., Kantoff, P.W., Wooster, R., Farokhzad, O.C., 2017. Cancer nanomedicine: progress, challenges and opportunities. Nat. Rev. Cancer 17, 20–37. https://doi.org/10.1038/nrc.2016.108

Sipponen, M.H., Lange, H., Crestini, C., Henn, A., Österberg, M., 2019. Lignin for Nano- and Microscaled Carrier Systems: Applications, Trends, and Challenges. ChemSusChem 12, 2039–2054. https://doi.org/10.1002/cssc.201900480

Slegers, M.F.W., Stroosnijder, L., 2008. Beyond the Desertification Narrative: A Framework for Agricultural Drought in Semi-Arid East Africa. Ambio 37, 372–380.

Soares, S., Sousa, J., Pais, A., Vitorino, C., 2018. Nanomedicine: Principles, Properties, and Regulatory Issues. Front. Chem. 6. https://doi.org/10.3389/fchem.2018.00360

Soppimath, K.S., Aminabhavi, T.M., Kulkarni, A.R., Rudzinski, W.E., 2001. Biodegradable polymeric nanoparticles as drug delivery devices. J. Control. Release Off. J. Control. Release Soc. 70, 1–20. https://doi.org/10.1016/s0168-3659(00)00339-4

Taghavi, S.M., Momenpour, M., Azarian, M., Ahmadian, M., Souri, F., Taghavi, S.A., Sadeghain, M., Karchani, M., 2013. Effects of Nanoparticles on the Environment and Outdoor Workplaces. Electron. Physician 5, 706–712. https://doi.org/10.14661/2013.706-712

Tanaka, Y., Kimura, T., Hikino, K., Goto, S., Nishimura, M., Mano, S., Nakagawa, T., 2012. Gateway Vectors for Plant Genetic Engineering: Overview of Plant Vectors, Application for Bimolecular Fluorescence Complementation (BiFC) and Multigene Construction, Genetic Engineering - Basics, New Applications and Responsibilities. IntechOpen. https://doi.org/10.5772/32009

Tang, Q., Qian, Y., Yang, D., Qiu, X., Qin, Y., Zhou, M., 2020. Lignin-Based Nanoparticles: A Review on Their Preparations and Applications. Polymers 12, 2471. https://doi.org/10.3390/polym12112471

Tian, D., Hu, J., Bao, J., Chandra, R.P., Saddler, J.N., Lu, C., 2017. Lignin valorization: lignin nanoparticles as high-value bio-additive for multifunctional nanocomposites. Biotechnol. Biofuels 10, 192. https://doi.org/10.1186/s13068-017-0876-z

Usman, M., Farooq, M., Wakeel, A., Nawaz, A., Cheema, S.A., Rehman, H. ur, Ashraf, I., Sanaullah, M., 2020. Nanotechnology in agriculture: Current status, challenges and future opportunities. Sci. Total Environ. 721, 137778. https://doi.org/10.1016/j.scitotenv.2020.137778

Waalewijn-Kool, P.L., Ortiz, M.D., Lofts, S., Gestel, C.A.M. van, 2013. The effect of pH on the toxicity of zinc oxide nanoparticles to Folsomia candida in amended field soil. Environ. Toxicol. Chem. 32, 2349–2355. https://doi.org/10.1002/etc.2302

Weir, I.E., 2001. Chapter 23 Analysis of apoptosis in plant cells, in: Methods in Cell Biology, Cytometry. Academic Press, pp. 505–526. https://doi.org/10.1016/S0091-679X(01)63027-9

Withers, P., Neal, C., Jarvie, H., Doody, D., 2014. Agriculture and Eutrophication: Where Do We Go from Here? Sustainability 6, 5853–5875. https://doi.org/10.3390/su6095853

Xia, T., Kovochich, M., Liong, M., Mädler, L., Gilbert, B., Shi, H., Yeh, J.I., Zink, J.I., Nel, A.E., 2008. Comparison of the Mechanism of Toxicity of Zinc Oxide and Cerium Oxide Nanoparticles Based on Dissolution and Oxidative Stress Properties. ACS Nano 2, 2121–2134. https://doi.org/10.1021/nn800511k

Yang, W., Owczarek, J.S., Fortunati, E., Kozanecki, M., Mazzaglia, A., Balestra, G.M., Kenny, J.M., Torre, L., Puglia, D., 2016. Antioxidant and antibacterial lignin nanoparticles in polyvinyl alcohol/chitosan films for active packaging. Ind. Crops Prod. 94, 800–811. https://doi.org/10.1016/j.indcrop.2016.09.061

Yang, Z., Mei, L., Xia, F., Luo, Q., Fu, L., Gong, H., 2015. Dual-slit confocal light sheet microscopy for in vivo whole-brain imaging of zebrafish. Biomed. Opt. Express 6, 1797–1811. https://doi.org/10.1364/BOE.6.001797

Yiamsawas, D., Baier, G., Thines, E., Landfester, K., Wurm, F.R., 2014. Biodegradable lignin nanocontainers. RSC Adv. 4, 11661–11663. https://doi.org/10.1039/C3RA47971D

Zhang, M., Viennois, E., Xu, C., Merlin, D., 2016. Plant derived edible nanoparticles as a new therapeutic approach against diseases. Tissue Barriers 4, e1134415. https://doi.org/10.1080/21688370.2015.1134415

Zhou, X., Liang, J., Liu, Q., Huang, D., Xu, J., Gu, H., Xue, W., 2021. Codelivery of epigallocatechin-3-gallate and diallyl trisulfide by near-infrared light-responsive mesoporous polydopamine nanoparticles for enhanced antitumor efficacy. Int. J. Pharm. 592, 120020. https://doi.org/10.1016/j.ijpharm.2020.120020

Zikeli, F., Vinciguerra, V., D'Annibale, A., Capitani, D., Romagnoli, M., Scarascia Mugnozza, G., 2019. Preparation of Lignin Nanoparticles from Wood Waste for Wood Surface Treatment. Nanomaterials 9, 281. https://doi.org/10.3390/nano9020281